Supplementary file S3 to: Grimm, V. et al. (2020) 'The ODD Protocol for Describing Agent-Based and Other Simulation Models: A Second Update to Improve Clarity, Replication, and Structural Realism' *Journal of Artificial Societies and Social Simulation* 23 (2) 7: http://jasss.soc.surrey.ac.uk/23/2/7.html [10.18564/jasss.4259]

S3: Nested ODD

[1]This supplement includes an example of a "nested ODD" where some submodels are so complex, and large, that by themselves their description uses some elements of ODD's structure, i.e. "Purpose", "Process overview and scheduling", and "Submodels". The example also demonstrates how to separate model equations from the main text by compiling them in tables.

The ODD below includes elements of earlier ODDs (see references below) and new elements, in particular regarding energy budgets of the species considered, the harbor porpoise. The ODD, and the corresponding model, were developed by Cara Gallagher, University of Aarhus, Department of Bioscience – Section for Marine Mammal Research, Denmark (cgallagher@bios.au.dk) and is a draft version of a supplement to Gallagher et al. (*unpubl. manuscript*). All section number start with "2." because this ODD is the second section of a corresponding TRACE document.

Section contents:

[1] Lead author of this supplement: Cara Gallagher.

The ODD protocol presented here includes elements from the model descriptions of four different harbor porpoise models. The original model (M1 and orange text) was developed to explicitly model the movements of porpoises in Danish waters (Nabe-Nielsen et al. 2013). The second model (M2 and green text) extended M1 by incorporating simplistic energetics and modelled the effects of anthropogenic noise and bycatch on the porpoise population in the inner Danish waters (Nabe-Nielsen et al. 2014). The third model (M3 and purple text) was developed as a further extension of the model into the North Sea, with area-specific large-scale movements and more realistic behavioral effects of disturbances (Nabe-Nielsen et al. 2018); it is important to note that the noise and transmission loss modelling from M3 was incorporated into the model presented here, but the movements were retained from M1 and M2, as these correspond to animals in the inner Danish waters. Text in black represents the current version of the model presented here (M4).

2.1 Purpose and patterns

The purpose of the model is to simulate the population dynamics of harbor porpoises, *Phocoena phocoena*, in the Inner Danish Waters (IDW), an environment with large seasonal fluctuations in temperature and salinity, and to investigate how energy budgets can be used to evaluate the seasonal variation in impacts of noise in this species, in particular seismic surveys. This model is an extension to a previously published IBM of harbor porpoises in the IDW (Nabe-Nielsen et al. 2013, 2014) as it represents the individual energetics of harbor porpoises in a more realistic manner. Our approach is based on first principles and explicitly accounts for variations in energy requirements among individual animals.

To evaluate if the model is producing realistic patterns, deeming it useful for its purpose, model outputs were compared to empirical data for porpoises in the IDW related to the blubber masses of different age and reproductive classes, seasonal shifts in blubber depth, total metabolic costs, energy intake, mass-length relationships, and age-class distributions of the population.

2.2 Entities, state variables, and scales

The model is composed of three kinds of entities: porpoise agents (called “porps”), disturbance agents (here ships), and landscape grid cells. As in Nabe-Nielsen et al. (2014), porp agents are characterized by their location, speed, movement direction, age, age of maturity, storage level, pregnancy status and lactation status (Table. 2.1.). Here we also include the state variables length, mass, blubber mass, and body condition. Porps are ‘super-individuals’ (Scheffer et al. 1995), hereafter referred to as individuals, that represent several female porpoises with characteristics aligning with those of porpoises in the IDW population. Ships are represented by their location, speed, movement direction, and noise level, as in Nabe-Nielsen et al. (2014). The simulated landscape is also conserved from Nabe-Nielsen et al. (2014) and covers a 240 km x 400 km area of the IDW centered around the islands Funen and Zealand (see Fig. 2.1). The landscape is composed of 600 x 1000 grid cells, each covering 400m x 400m.

Each landscape grid cell is characterized by its location, average water depth, distance to land, food level and maximum food level (as in Nabe-Nielsen et al. 2014) (Table. 2.2.); in this study we introduce the state variables location-specific water temperature and salinity to allow for spatiotemporally specific calculation of the thermophysical parameters involved in

metabolic calculations. Grid cells are divided into land (52.1%), water without food (47.1%), and randomly distributed food patches (4572 individual patches) (0.76%), as in Nabe-Nielsen et al. (2014). The maximum food level for each food patch was estimated by assuming that its food level correlated with the probability of porpoise presence as determined by maximum entropy (MaxEnt) estimates of porpoise distribution for animals tagged with satellite transmitters (Edrén et al. 2010, Nabe-Nielsen et al. 2014). There is no food outside of food patches. The porps' large-scale movements are guided by the maximum season-specific food level in different 40km x 40km squares, called "blocks".

The model proceeds in discrete time steps of 30-minutes and typically runs for 20 years. Each month consists of 30 days and a year of 360 days. Metabolic calculations are in units of energy per unit time (J $30min^{-1}$).

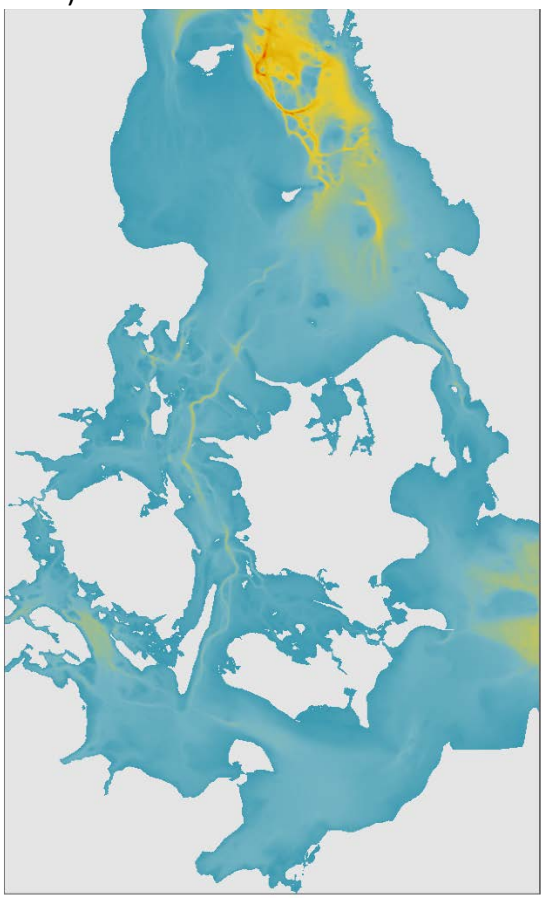

Fig. 2.1. Model landscape extent (grey: land; water color gradient displaying bathymetry with shallow water in blue and deep water in red).

Table 2.1. Porps in the model are described by state variables related to their morphometrics, physiology, and reproductive state.

Symbol	Code	Description [units]
State variables of all porps:		
m	weight	Mass [kg]
m_{str}	m_Struct	Mass of structural (non-storage) tissues [kg]
L	lgth	Body length* [m]
age	age	Age in years [years]

V_{bl}	v_Blub	Blubber volume [cm^3]
$V_{\mathrm{bl,min}}$	v_Blub_min	Blubber volume with 100% probability of mortality* [cm^3]
$V_{\mathrm{bl,R}}$	v_Blub_repro	Threshold blubber volume for reproductive investment* [cm^3]
SL	Storage_Level	Storage level*; blubber mass as a proportion of total mass [%]
SA	SA	Surface area* [m^2]
ps	pregnancyStatus	Pregnancy status [1, 2, or 3]
ls	With_Lact_Calf	Lactation status [true or false]
w_{sf}	wean_Scale_Fact	Weaning scale factor*; calf dependency on milk [%]
$d_{\mathrm{B,site}}$	-	Blubber depth at each of 9 body sites* [cm]
M_{B}	m_BMR	Basal metabolic rate* [J $30min^{-1}$]
M_{L}	m_Loco	Metabolic cost of locomotion* [J $30min^{-1}$]
M_{T}	m_Thermo	Metabolic cost of thermoregulation* [J $30min^{-1}$]
T_{S}	t_Skin	Skin temperature* [C]
M_{G}	m_Growth	Metabolic cost of growth* [J $30min^{-1}$]
V	swimspeed	Swimming speed [m s^{-1}]
For pregnant or lactating females:		
m_{f}	mass_F	Mass of fetus [kg]
m_{calf}	mass_C	Mass of lactating calf [kg]
$m_{\mathrm{str,calf}}$	m_Struct_Calf	Structural mass of lactating calf [kg]
L_{calf}	lgth_Calf	Body length of lactating calf* [m]
$V_{\mathrm{bl,calf}}$	v_Blub_Calf	Blubber volume of lactating calf [cm^3]
$V_{\mathrm{bl,c,idl}}$	v_Blub_Calf_Idl	Ideal blubber volume of lactating calf*; based on mean empirical *SL* [cm^3]
sex_{c}	sex_Calf	Sex of lactating calves [“male” or “female”]
SA_{c}	SA_Calf	Surface area of lactating calf* [m^2]
$M_{\mathrm{B,calf}}$	m_BMR_Calf	Basal metabolic rate of lactating calf* [J $30min^{-1}$]
$M_{\mathrm{T,calf}}$	m_Thermo_Calf	Metabolic cost of thermoregulation of lactating calf* [J $30min^{-1}$]
$M_{\mathrm{G,f}}$	m_Growth_F	Metabolic cost of growth of fetus* [J $30min^{-1}$]
$M_{\mathrm{G,calf}}$	m_Growth_Calf	Metabolic cost of growth of lactating calf* [J $30min^{-1}$]
M_{P}	m_Preg	Metabolic cost of pregnancy* [J $30min^{-1}$]
M_{Lact}	m_Lact_Real	Realized metabolic cost of lactation* [J $30min^{-1}$]
ds_{mating}	ds-mating	Days since mating [days]
ds_{birth}	dsg-birth	Days since giving birth [days]

*Deduced state variables (calculated using other state variables)

Table 2.2. The modeled grid cells are characterized by environmental parameters and state variables related

to the season and the location of the grid cell. State variables related the thermophysical properties of water are used for the calculation of energy budgets.

Environmental parameters:

Symbol	Value	Code	Description [units] (reference)
r_U	0.1	food-growth-rate	Food replenishment rate [unitless] (Nabe-Nielsen et al., 2013)
$U_{\max}$	1	U_max	Maximum food content in a patch (Nabe-Nielsen et al. 2014)
$U_{\min}$	0.1	-	Minimum food content in a patch (Nabe-Nielsen et al. 2014)

State variables:

Symbol	Code	Description [units]
$U[c]$	food-level	Food level of a patch [food units]
$T_{\mathrm{W}}[c]$	temp_W	Location specific water temperature [C]
$S_{\mathrm{W}}[c]$	salinity_W	Location specific water salinity [psu]
$\rho[c]$	density_W	Water density* [kg m^{-3}]
$k_{\mathrm{W}}[c]$	conductivity_W	Conductivity of water* [W C^{-1} m^{-1}]
$c_{\mathrm{P}}[c]$	specHeat_W	Specific heat capacity of water* [kJ kg^{-1} K^{-1}]
$\beta[c]$	CoeffofThermalExpansion_W	Coefficient of thermal expansion* [C^{-1}]
$\mu[c]$	dynamicVis_W	Dynamic viscosity of water* [kg m^{-1} s^{-1}]
$Pr[c]$	Pr_W	Prandtl number* [unitless]
$\nu[c]$	kinVisc_W	Kinematic viscosity* [m^2 s^{-1}]

*Deduced state variables (calculated using other state variables)

2.3 Process overview and scheduling

M2: At the beginning of each timestep porps move and respond to noise by adjusting their movements if disturbed (*Movement*) (see Fig. 2.2 for visual process overview). The movement model includes memory of favorable patches to which movement is oriented when moving in unfavorable locations. Thereby, dynamic homeranges emerge, reflecting the distribution of resources and conspecifics. If an animal's storage level has decreased for 3 days, it switches to large-scale movements. These movements aren't affected by noise.

After moving, porps ingest and expend energy on their metabolic costs (*Energy budget*). Energy is ingested and assimilated from prey patches if available. Assimilated and stored energy are used to allocate to metabolic processes in order of importance to survival, following Sibly et al. (2013). Any energy remaining after fulfilling costs is stored as blubber, affecting the storage level of the animal.

M1: The food levels in the patches are dynamically changing. When a patch is visited by a porp its food level drops corresponding to the amount consumed by the porp, but afterwards it increases logistically in daily steps until reaching the maximum food level for the patch. M2: Whereas the logistic food growth rate is kept constant, the maximum food level in a patch depends on the time of the year and on where it is located. The season-specific maximum food level was obtained from maximum entropy (MaxEnt) estimates of where porpoises are most likely to occur (Edrén et al., 2010). These were calculated from the

number of observations of satellite-tracked animals in areas with different environmental conditions.

Once every day porps may die (with probabilities that depend on their energy level and age), mate, become pregnant, give birth, or wean a calf (depending on the time of the year and reproductive status; submodel *Life-history*).

Environmental parameters, such as water temperature and salinity, are updated monthly (on the 1st day of each month) and correspond to location-specific monthly averages from the Copernicus database for 2007-2016 (http://marine.copernicus.eu). The thermophysical properties of seawater are then determined for each patch using lookup tables specific to each temperature and salinity combination. The formulae used to determine the values used in the lookup tables can be found in Table 3.3 in TRACE section 3.

M2: If day of year is 60, 150, 210 or 300: Season-specific MaxEnt data are updated. Between days 300 and day 60 (i.e. during winter): the values are rescaled to lie in the range 0–1. For other seasons: values are rescaled to achieve the same potential food level for the entire landscape (to ensure that the sum of the maximum food levels for all patches does not change among seasons). If the day of year is 1: each porp calculates a new mating date.

The porp agents' blubber mass depends on their movements, morphometrics (size and shape), and reproductive state. State variables related to morphometrics (V_{bl}, m, SA, SL) and IR_{max} are updated at the end of every time step (30 minutes; Table 2.1.), while other variables are updated asynchronously; i.e. immediately after execution of their related process. Body site-specific blubber depth, $d_{\mathrm{B,site}}$, and age are updated once per day.

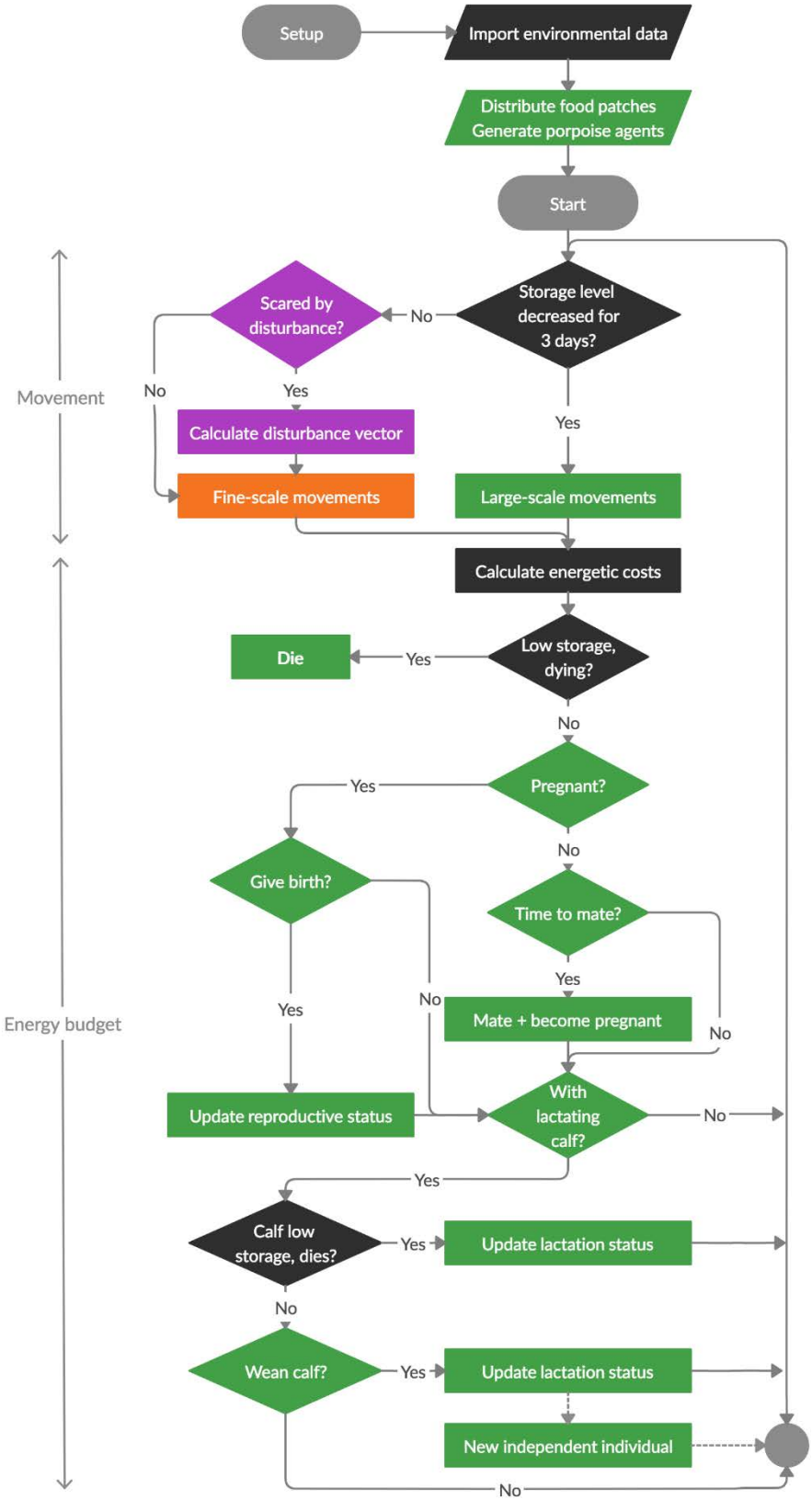

Figure 2.2. Flow diagram describing the details of the population portion of the model. Only adult females are modelled explicitly. Diamond-shaped symbols indicate decisions made by porps, parallelograms indicate model input/output and rectangles indicate calculations. Color indicates where each process was conserved from (Nabe-Nielsen et al. 2013 in orange; Nabe-Nielsen et al. 2014 in green; Nabe-Nielsen et al. 2018 in purple; and the current model in black). A detailed description of all elements of this flow diagram can be found in the movement and energy budget submodel descriptions.

2.4 Design concepts

Basic principles:

This model is built on the assumptions that the porpoise population in the IDW is food limited and that noise affects porpoises by displacing them from specific regions, hence reducing their food intake. Energy budgets are based on physiological principles (Sibly et al. 2012, Sibly et al. 2013) and mathematical models of energy expenditure (Hind and Gurney 1997, Gallagher et al. 2018). This model builds on the ability of animals to make behavioral and reproductive decisions based on memory (Van Moorter et al. 2009) and current body condition, such as when to move to a previously visited food patch or move to a new region or when to abort or abandon calves.

Emergence:

Population size and demographics emerge from adaptive decisions made by porps related to their movements and energetic state, which have the potential to ultimately improve individual fitness. The realized growth rates of individuals, age at first successful reproduction, and body condition are emergent properties of the model and affect the size and demographics of the population. While the use of a pregnancy rate imposes a maximum cap on the annual reproductive effort, the actual number of calves born in a year emerges from the current environmental and physiological state of females. Age-related and seasonal fluctuations in body condition emerge from variations in foraging efficiency and environmental conditions experienced by porps. While the potential maximum energy taken in in a timestep is modified using a water-temperature based modifier, the total energy consumed and stored is based on the resources encountered and the energetic costs experienced by animals. The relationship between mortality probability and storage level is imposed but an animal's probability of dying at any point in time is driven by the storage level, which emerges from the animal's foraging success. The spatial distribution and home ranges of porps in the model emerge from the way individuals move in response to changing energy levels.

Objectives:

Animals attempt to maximize their fitness by maximizing energy intake through memory-based movement and by allocating available energy to processes in order of necessity. If processes necessary to survival are not covered by energy intake, stored energy will be used to cover them. As storage levels decrease, the animal has an increasing probability of dying. Processes not critical to immediate survival can be left unmet with some trade-off occurring (Sibly et al. 2013), such as reduced growth or calf loss.

Prediction:

Animals base their prediction of how much food they can gather in different food patches on their previous visits to those patches, and this influences their fine-scale movements. Their memory, though, is limited and, after some time, patches visited in the distant past are forgotten. Animals are assumed to have knowledge about which parts of the landscape have the highest food levels at different times of the year. This permits them to move to one of the 40 km × 40 km blocks with the highest potential food level when using large-scale movements.

Sensing:

Porps can sense their storage levels and make decisions specific to their current state, e.g. move to higher quality areas, reduce reproductive investment, or use energy converted from

stores. They can sense water depth and temperature. Sensing water depth allows them to turn away from coast lines. Porps can also sense noise levels from ships and turbines, and this affects their movements.

Interaction:
The porps only interact indirectly by foraging on the same food patches. Once they begin to take solid foods (beginning at 3mo) dependent calves foraging in the same patches also compete with their mothers.

Stochasticity:
Fine-scale movements, individual morphometrics, energetic inputs, mortality, and dates related to reproduction (e.g. mating date, calving date, and date of weaning) are associated with stochasticity in the model (see Table 3.1). In all these cases, the variation represented is considered important, as it may have consequences, but its mechanistic basis is unknown or considered not relevant for the purpose of the model. The probability of surviving increases with increasing energy levels.

Collectives:
Mothers and dependent calves in the model act as collectives. They move and forage as one unit. Super-individuals represent approximately 100 individual porpoises, assessed using the latest population counts (SCANS III, 2016), but their energetics are modelled to resemble the energetics of a single animal; they were introduced for run-time reasons and to represent densities which are typical of the IDW.

Observation:
The number of animals, their storage levels, and the total amount of food in the landscape are recorded daily. Age-class distributions and age-specific mortalities are recorded yearly.

2.5 Initialization

The model is by default initialized by creating 200 randomly distributed female porp individuals, representing 20,000 real porpoises. Their age-class distribution corresponds to that of stranded and bycaught animals (Lockyer & Kinze 2003) and 67% of the adults are pregnant. No porps are initialized with lactating calves. Their initial morphometric state variables (length, mass, storage level, and site-specific blubber depth) correspond to those of by-caught female porpoises from the Inner Danish and nearby waters (unpublished data from C. Kinze & A. Galatius (IDW porpoise dataset)) (TRACE Section 3 Table 3.3). Mating, calving, and weaning periods of the individuals were set to occur at day 225 (±20), day 182 (±20), and day 60 (±20), respectively (mean ±SD; random normal variables; Lockyer & Kinze 2003, Lockyer 2003, Nabe-Nielsen et al. 2014). Simulations were initiated on 1 January and food levels in food patches were initialized as the location specific maximum food levels for that date. Location-specific environmental parameters were taken as the average found for the month of January from the Copernicus dataset for the years 2007–2016. If running simulations, survey ships are initialized and the XY positions of the “buoys” used as turning points for the vessels to follow the survey route are loaded at setup. Parameters related to noise and disturbance can be chosen on the user interface, with defaults found in the Movement model parameter table (Table 2.3.).

The procedures involved in initialization are:

- Setup
- Setup_Global_Parameters
- Landsc_Setup
- Porps_Setup
- Update_Block_Values
- Ships_Setup

In the Setup procedure, which is called by the UI "Setup" button, the world is cleared and completely reset, aside from the interface slider values. In the Setup_Global_Parameters procedure all global parameter values, e.g. constants such as the energy densities of tissues, gestation and lactation period length, etc., are set. In Landsc_Setup procedure, all environmental parameters are set up and maps are imported. In Porps_Setup, the model first sets up porp parameters and then assigns their state variables. After Porps_Setup, the Update_Block_Values procedure is run to initialize the mean MaxEnt values for blocks for each quarter. If a scenario is selected using the Netlogo "chooser" scenario, and a scenario month and scenario order (for Scenario 2) are selected using the "sc_month" and "sc_order" choosers, the survey ships are then setup using the Ships_Setup procedure.

2.6 Input data

Seven types of background maps are used in the model. The food probability (a binomial 0 or 1 value) is determined using the file 'patches.asc'. The bathymetry and distance to coast for patches is set using the files 'bathy.asc' and 'disttocoast.asc', respectively, and block number is determined using the file 'blocks.asc'. The maximum food level of a food patch was obtained from seasonal MaxEnt estimates, as in Nabe-Nielsen et al. (2014) (ascii files: 'quarter'1-4'.asc'). Environmental conditions, like water temperature and salinity, were obtained from the Copernicus database Baltic Sea Reanalysis Product for years 2007-2016 and updated once a month (ascii files: 'TempData_Month'X'.asc' & 'SalData_Month'X'.asc') (see TRACE Data Evaluation for more information on temperature and salinity maps). All ascii maps used have a spatial resolution equal to the patch size of 400m × 400m, however, as the dataset used to create the temperature and salinity maps has a spatial resolution of 4km × 4km, patches falling within each 4km × 4km contain identical temperature and salinity values.

For each patch, the thermophysical properties of seawater (i.e. water density, thermal conductivity, coefficient of thermal expansion, specific heat capacity, dynamic viscosity, Prandtl number, and kinematic viscosity) are pulled from lookup tables (loaded at setup and stored as global matrices) once a month following the temperature and salinity map update using the location-specific water temperature and salinity values (in the 'thermophysical properties of SW tables' folder: 'DensityTable.csv', 'ThermalConductivity.csv', 'SpecificHeat.csv', 'CoefOfThermalExpansionTable.csv', & 'DynamicVis.csv'). The Prandtl number, Pr, and kinematic viscosity of water, ν, are then determined using these values (see TRACE Section 3 Table 3.4 for details).

Simulations include details for simulating disturbance from seismic surveys. These details are provided in a txt file with the location identifier of the survey route, x,y coordinates of navigation buoys, source level, and start and end timestep of the survey. Noise is emitted for all timesteps where a survey vessel is present. The source level of all surveys was taken as 262 dB re 1 µPa peak-peak (a standard metric for noise levels in water; Thomspson et al.

2013, Kyhn et al. 2019). The threshold where a behavioral reaction occurred was set at 165 dB re 1 µPa peak-peak corresponding to the minimum distance recorded to result in a behavioral reaction in wild porpoises responding to a commercial seismic survey in Thompson et al. (2013). See the Movement model for details on how noise from seismic survey ship agents was represented in the model.

2.7 Submodels

As the model described is composed of two distinct submodels, the Movement and Energy budget models, here we use a "Nested ODD" structure to allow for thorough description of each model. For each, the *Purpose*, *Process overview & scheduling*, and "*Sub-submodels*" will be presented in detail. Equations used in these submodels are listed in tables and are linked, via hyperlinks to the NetLogo code provided in a separate document. (Note that hyperlink forward and backward navigation work via the key combinations "Alt"+right/left arrow key) as well as via comments in the NetLogo code referring the number of the equation implemented. All parameters used in our model are listed in this Section, but divided into partial tables with parameters related to specific processes.

2.7.1 Movement model

The movement model used here was developed in Nabe-Nielsen et al. (2013) and employed in Nabe-Nielsen et al. (2014) and is based on memory-based adaptive foraging behavior. This model was informed and calibrated using movement track data from porpoises in the inner Danish waters (Sveegaard et al. 2011).

2.7.1.1 Purpose

The Movement model allows for porps to make adaptive movement decisions based on spatial memory and their current energetic state and to sense and respond to anthropogenic disturbances.

2.7.1.2 Process overview & scheduling

M2: The animals' *fine-scale movements* are controlled by a combination of correlated random walk (CRW) behavior (Turchin, 1998) and a tendency to move towards patches where they previously found food; this tendency is represented by a vector calculated from memorized food patches, where the memory decays with a certain rate. The contribution of the CRW behavior is controlled by the amount of food found in the recent past. If the fine scale movements do not allow them to sustain their storage level, they switch to *large-scale movements* to move towards blocks with high potential food levels. The large-scale movement speeds and routes resemble those in satellite-tracked animals (Sveegaard et al., 2011). Porps whose energy levels were higher in the previous week turn back to where they then foraged. Turns are also made if there is land ahead or if ships are close, particularly if these have high noise levels (that is, the porps get scared by noise; *deterrence behavior*). The porps remain scared for 2.5 h, but the extent to which they are scared is halved at every time step. The animals move one at a time in an order that is randomized after each half-hour time step.

If seismic survey ships are present, they move along their survey routes at constant speeds and emit constant source levels. When ships reach each navigation buoy, they set their heading towards the next buoy. When they reach their final buoy, they disappear.

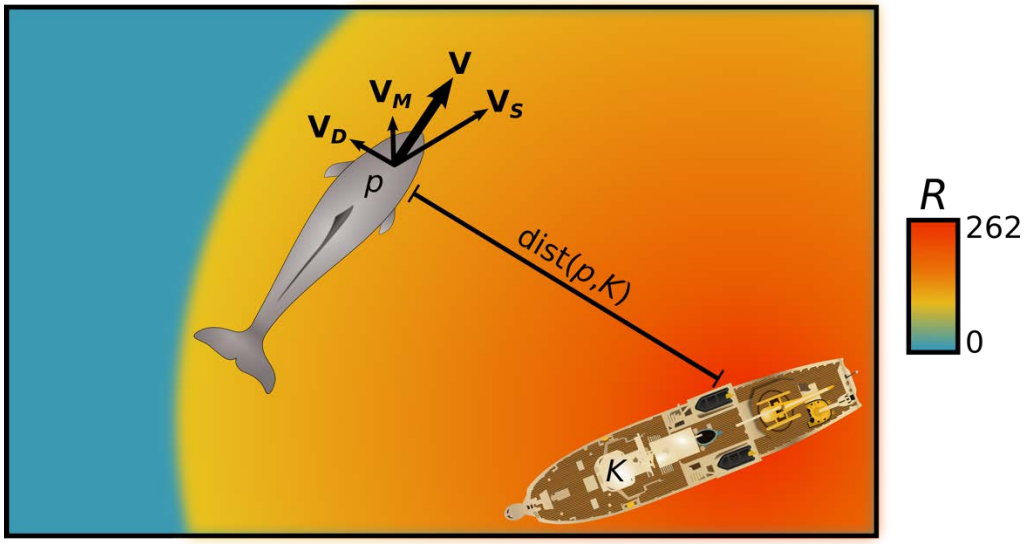

Figure 2.3. Effects of noise on porp movement in the model. Vector $\mathbf{V}_S$ represents the correlated random walk during one 30-min time step and $\mathbf{V}_M$ represents the spatial memory vector. Vector $\mathbf{V}_D$ displays the movement vector that is produced exclusively by the reaction to noise. The length of $\mathbf{V}_D$ is determined by the received sound level (*RL*), which decreases logarithmically with distance from the sound source. Vector **V** is the vector resulting from the combined effect of movement vectors $\mathbf{V}_S$, $\mathbf{V}_M$, & $\mathbf{V}_D$ and represents the actual step taken by the porp in the presence of noise.

2.7.1.3 Sub-submodels

Table 2.3. Parameters used in the movement model.

Symbol	Value	Code	Description [units] (reference)
r_R	0.20	rR	Reference memory decay rate; determines how fast the animals forget the location of previously visited food patches [unitless] (Nabe-Nielsen et al. 2014)
r_S	0.10	rW	Satiation memory decay rate; determines how fast the animals get hungry after eating [unitless] (Nabe-Nielsen et al. 2014)
a	0.94	corr-logmov	Autocorrelation constant for $\log_{10}$(d /100) where d is distance moved [m] per 30 min (Nabe-Nielsen et al. 2013)
b	0.26	corr-angle	Autocorrelation constant for turning angles (Nabe-Nielsen et al. 2013)
R_1	N(0.42, 0.48)*	R1	Log_{10} distance moved per time step (mean ± 1 SD) [m] (Nabe-Nielsen et al. 2013)
R_2	N(0, 38)*	R2	Turning angles between steps (mean ± 1 SD) [deg] (Nabe-Nielsen et al. 2013)
NSL	262	source_Level	Disturbance source level [dB re 1 µPa peak-peak] (Thompson et al. 2013, Kyhn et al. 2019)
T	165	resp_Level	Response threshold [dB re 1 µPa peak-peak] (Thompson et al. 2013)
c	0.7	deterrence_Coeff	Deterrence coefficient [unitless] (Nabe-Nielsen et al. 2018)
t_{deter}	5	deter_Time	Deterrence time [timesteps] (Nabe-Nielsen et al. 2014)
w_{disp}	4	min_Disp_Depth	Minimum water depth when using large-scale movements [m] (Nabe-Nielsen et al. 2014).
w_{min}	1	min_Depth	Minimum water depth [m] required by porpoises (J. Tougaard, pers. obs).
q	12	n_Disp_Targets	Number of potential large-scale movement targets = 40×40 km blocks [#] (Nabe-Nielsen et al. 2014).
d_{disp}	1.6	mean_Disp_Dist	Length of large-scale movement time steps [km 30min^{-1}] (J. Teilmann, unpublished satellite data).
Transmission loss models used in scenarios:			
Site [#]:	$\hat{\beta}$	$\hat{\alpha}$	Reference:

Omø [1]	16.7	0.00086	Barham, 2016
Sejerø Bugt [2]	18.7	0.000343	NIRAS, Rambøll, and DHI, 2015
Samsø [3]	17.7	0.0006	Average of other two sites

*Normal distribution with mean and standard deviation

Table 2.4. Equations used in the fine-scale movement model.

Eqn#	Function [units]	Code	Symbol	Equation	Source
1	Combined CRW and spatial memory movement vectors [Δxy]	vt	s_t	$\mathbf{V}_S + \mathbf{V}_M$	Nabe-Nielsen et al. 2013
2	CRW vector [Δxy]	CRW-contrib	$\mathbf{V}_S$	$x_t(k + E_t)$	Nabe-Nielsen et al. 2013
3	Spatial memory vector [Δxy]	vt	$\mathbf{V}_M$	$\sum_c R[c]_t \, i[c]_t$	Nabe-Nielsen et al. 2013
4	Expectation of patch profitability [food units]	perceived-util-list	$R[c]_t$	$\frac{M_R[c]_t \times U[c]}{D[c]_t}$	Nabe-Nielsen et al. 2013
5	Reference memory [unitless]	ref-mem-strength-list	$M_R[c]_{t+1}$	$M_R[c]_t - r_R \times M_R[c]_t \times (1 - M_R[c]_t)$	Nabe-Nielsen et al. 2013
6	Expectation of CRW profitability [food units]	VE-total	E_t	$\sum_c M_S[c]_t \times U[c]$	Nabe-Nielsen et al. 2013
7	Distance moved in CRW [400m]	pres-mov	δ_t	$R_1 + a\delta_{t-1}$	Nabe-Nielsen et al. 2013
8	Turning angle in CRW [θ]	prev-angle	ψ_t	$R_2 - b\psi_{t-1}$	Nabe-Nielsen et al. 2013
9	Received sound level [dB re 1 µPa peak-peak]	rec_Level	R	$NSL - \hat{\beta}\log_{10}(\mathrm{dist}(p,K)) + \hat{\alpha}(\mathrm{dist}(p,K))$	Urick 1983
10	Maximum disturbance distance [m]	deter_Dist	$dist_{\max}$	$10^{(NSL-T)/X}$	Nabe-Nielsen et al. 2018
11	Length of the disturbance vector [Δxy]	deter_Vt	$\mathbf{V}_D$	$c(R - T)$	Nabe-Nielsen et al. 2018
12	Realized movement vector [Δxy]	total_Dx & total_Dy	$\mathbf{V}^*$	$\frac{\mathbf{V}_M + \mathbf{V}_S + \mathbf{V}_D}{\lVert\mathbf{V}_M + \mathbf{V}_S + \mathbf{V}_D\rVert} \times \lVert\mathbf{V}_S\rVert$	Nabe-Nielsen et al. 2018

×

2.7.1.3.1 Fine-scale movements - Spatial memory and correlated random walk

M1: The direction of the move s_t from time t to time $t + 1$ is calculated from the sum of two vectors corresponding to the two terms in Equation 1, where the first term represents a weighed CRW ($\mathbf{V}_S$) (Eqn. 2) and the second represents a spatial memory move ($\mathbf{V}_M$) (Eqn. 3). The animal's tendency to move according to the CRW depends on a short-term memory of how much food it has eaten in the recent past, that is, how satiated it is, and a constant k. Here k can be interpreted as the animal's tendency to keep moving following its intrinsic behavior irrespective of the amount of food acquired. The unweighted correlated random walk move is described by the vector x_t. The animal's tendency to move towards previously visited food patches depends on how profitable it expects it to be to return to each of them, $R[c]_t$. The $i[c]_t$ are unit vectors pointing towards each of the locations the animal has visited in the past. The sum of the individual attraction vectors is a spatial memory vector that points towards the area that the animal expects to be most rewarding based on previous experiences.

M1: *Assessing the benefit of returning to previously visited food patches*: An animal's expectation of how profitable it would be to return to a place where it has been before, $R[c]_t$, is modeled to depend on its ability to remember the place, $M_R[c]_t$, but also on how much food it found there, $U[c]$, and how costly it would be to return to it (Eqn. 4), where $D[c] > 1$. Both $U[c]$ and $D[c]$ could be measured in terms of the amount of energy used or obtained, and $M_R[c]$ is unitless. The animal's ability to remember places is modeled using a spatial memory, or reference memory, M_R. We let M_R decrease logistically with time, following Van Moorter et al. (2009) (Eqn. 5), where the shape of the logistic curve is determined by the reference memory decay rate, r_R.

M1: *Assessing the benefit of using an undirected search for food*: In our model we let the animals' memory of the food they have found in the recent past be determined by the short-term satiation memory, M_S. We let M_S decay following the same logistic equation as M_R (Eq. 5), but let its shape be controlled by the satiation memory decay rate, r_S, where $r_S > r_R$. The animal's expectation of how profitable it is to move at random can then be described using the amount food found at patches in the recent past, $U[c]$, and the memory of those patches, $M_S[c]$ (Eqn. 6).

M1: *Correlated random walk model*: An animal that exclusively follows its intrinsic behavior moves the step x_t during the period t to $t + 1$. Here all time steps have the same length (30 minutes). We let the distance moved during this time step, δ_t, correlate positively with the distance moved in the previous time step, δ_{t-1}, the stochastic variable R_1, and the positive constant a (Eqn. 7). Further, we let the turning angle ψ_t at time t be negatively correlated with the previous turning angle, ψ_{t-1}, and the positive constant b, and adjusted by the stochastic variable R_2 (Eqn. 8).

2.7.1.3.2 Deterrence behavior

M3: At the beginning of each time step, porps register anthropogenic noise. This is done by letting the noise source agents emit noise, thus producing a dynamic soundscape, which is updated every timestep where noise source agents are present. Noise source levels (NSL), positions and timings of disturbance events are provided as input data. Animals react to noise only up to a certain distance from a disturbance event. This distance is determined by the response threshold T and the extent to which sound is transmitted in water. Here T was determined based on studies of negative reactions (fleeing) in porps in response to seismic surveys (Thompson et al. 2013) and was set at 165 dB re 1 µPa peak-peak. The sound level received by the animals (R) was modeled using site-specific parameters models (Barham, 2016, NIRAS, Rambøll, and DHI, 2015), and logarithmic transmission loss (Eqn. 9). The sound level received by a porp depends on the distance from the porp p to the disturbance event K, $\mathrm{dist}(p, K)$. Noise emitted only influences animals out to a certain distance, $dist_{\max}$, where $R = T$ (Eqn. 10).

Each disturbance event equips all porp within the distance $dist_{\max}$ with a deterrence vector that points directly away from the noise source (Figure 2.3.). The length of the deterrence vector $\mathbf{V}_D$ is determined using the difference between the received sound level (R) and the response threshold (T) multiplied by the deterrence coefficient, c, assuming a linear relationship between the received sound level and the strength of reaction (Eqn. 11). Here for the deterrence coefficient, c, we used the value from Nabe-Nielsen et al. (2018) of c =0.07. Each animal's fine-scale movements are only influenced by the noise source that

yields the largest deterrence vector. When $\mathrm{dist}(p, K) > dist_{\max}$ the length of the deterrence vector is therefore set to 0.

2.7.1.3.3 Calculate combined step

M3: The vector describing the next fine-scale move (without considering land), $\mathbf{V}^*$, is determined by the spatial memory contribution, $\mathbf{V}_M$, the CRW contribution, $\mathbf{V}_S$, and the deterrence behavior contribution, $\mathbf{V}_D$. The length of the step is determined by the length of the CRW contribution, $||\mathbf{V}_S||$ (Eqn. 12). Here $\mathbf{V}^*$ has been standardized to have the same length as $\mathbf{V}_S$, so the length of the step is not affected by the noise level.

M3: If the move defined by $\mathbf{V}^*$ would cause the porp to move to an area with too shallow water ($<w_{\min}$) it turns in the direction with deepest water (40°, 70°, 120°, or 180° as needed).

2.7.1.3.4 Large-scale movements and back-tracking behavior

Each porp checks once per day whether it should switch to using large-scale movements:
M2: If its energy level has decreased for three days in a row, switch to large-scale movements. Turn towards a 40×40 km block selected at random among the q blocks where food patches have the highest average maximum food level. If its energy level was higher 6–9 days ago than over last three days and the porp is not using large-scale movements, switch to back-tracking movements. If the porp is already using large-scale movements, but this does not enable them to move to an area with sufficiently deep water ($>w_{disp}$), or if they are getting close to the target block, they should turn 180° relative to the place where they were one day earlier and then switch to back-tracking movements. If the porp's energy level becomes higher than at any point in the previous week, or if it gets trapped in an area with low water, it switches back to using fine scale-movements. Animals that use back-tracking movements turn ≤20° in the direction with deepest water at the beginning of each time step. If the animal is still in shallow water (< minimum depth) or <2 km from the coast it turns ≤30° away from land. Back-tracking turn up to 80° to at every time step to get to or remain at a distance of 1–4 km from land. The back-tracking behaviour enables simulated porps to move realistically between different parts of the simulated inner Danish waters landscape. Animals that are using large-scale or back-tracking movements move d_{disp} in each time step.

2.7.2 Energy budget model

The energy budget submodel developed here serves as an application and extension of the equation-based model in Gallagher et al. (2018) within an individual-based populations model. It is based on established general principles of physiological ecology. The model combines elements of the methods presented in Sibly et al. (2013) and Hind and Gurney (1997) to mechanistically model the energetic requirements of marine homeotherms. Sibly et al. (2013) serves as the foundation for the model framework and the allocation process follows this approach while the methods employed to model hydrodynamic and thermal processes follow those of Hind & Gurney (1997).

Table 2.5. State variables necessary for each of the energy budget sub-submodels. A filled in square represents the use of that state variable in the calculation of the sub-submodel. Squares in blue represent porp state variables while squares in green represent environmental state variables.

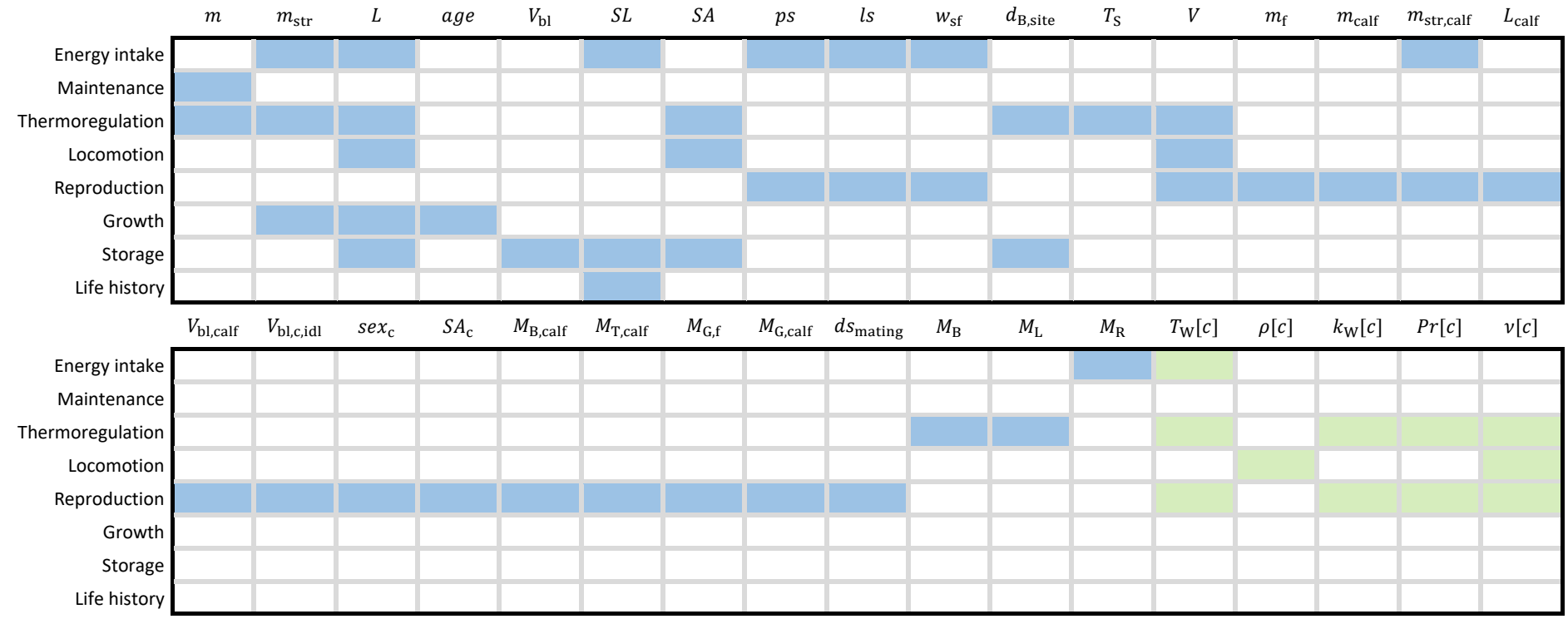

State variable definitions:

m	Mass	w_{sf}	Weaning scale factor	$V_{bl,c,idl}$	Ideal blubber volume of lactating calf	M_B	Basal metabolic rate
m_{str}	Mass of structural tissues	$d_{B,site}$	Body site-specific blubber depth	sex_c	Sex of lactating calves	M_L	Metabolic cost of locomotion
L	Body length	T_S	Skin temperature	SA_c	Surface area of lactating calf	M_R	Metabolic cost of reproduction
age	Age in years	V	Swimming speed	$M_{B,calf}$	Basal metabolic rate of lactating calf	$T_W[c]$	Water temperature
V_{bl}	Blubber volume	m_f	Mass of fetus	$M_{T,calf}$	Metabolic cost of thermoregulation of lactating calf	$\rho[c]$	Water density
SL	Storage level	m_{calf}	Mass of lactating calf	$M_{G,f}$	Metabolic cost of growth of fetus	$k_W[c]$	Conductivity of water
SA	Surface area	$m_{str,calf}$	Structural mass of lactating calf	$M_{G,calf}$	Metabolic cost of growth of lactating calf	$Pr[c]$	Prandtl number
ps	Pregnancy status	L_{calf}	Body length of lactating calf	ds_{mating}	Days since mating	$\nu[c]$	Kinematic viscosity
ls	Lactation status	$V_{bl,calf}$	Blubber volume of lactating calf				

2.7.2.1 Purpose

This model links the spatiotemporal variability in environmental conditions to the energy balance, survival probabilities, and reproductive success of cetaceans to be used as a tool in assessing the population level impacts of anthropogenic disturbance with high spatiotemporal resolution.

2.7.2.2 Process overview & scheduling

As the porps move, they acquire and assimilate energy from food patches (*Energy-intake*). Individuals then calculate their energy budgets (*Energy expenditure submodels*). Assimilated energy is expended on fulfilling their energy needs in the order of priority outlined in Fig. 2.4; *Maintenance*, *Thermoregulation*, *Locomotion*, *Reproduction*, and *Growth* and *Storage* (*Storage: Storing energy*). Due to the importance of blubber for marine mammals (Ryg et al. 1988; 1993), *Growth* and *Storage* are equally prioritized, meaning that any assimilated energy remaining after fulfilling other costs is split equally between them. If the *Growth* requirement is completely fulfilled and excess energy remains, it is diverted to storage. When the amount of energy available for allocation is not adequate to cover energetic requirements, stored blubber can be mobilized to meet those requirements (*Storage: Mobilizing storage*). Under conditions of low energy intake, several processes can be negatively affected. For calves and juvenile porps, low energy intake will first cause a slowing of growth and then a decrease in body condition which could ultimately lead to death. For reproductive females, insufficient energy intake can result in abortion or death of dependent calves, or in decreased body condition or death. See Table 2.5 for an overview of the state variables involved in each of the energy budget submodels.

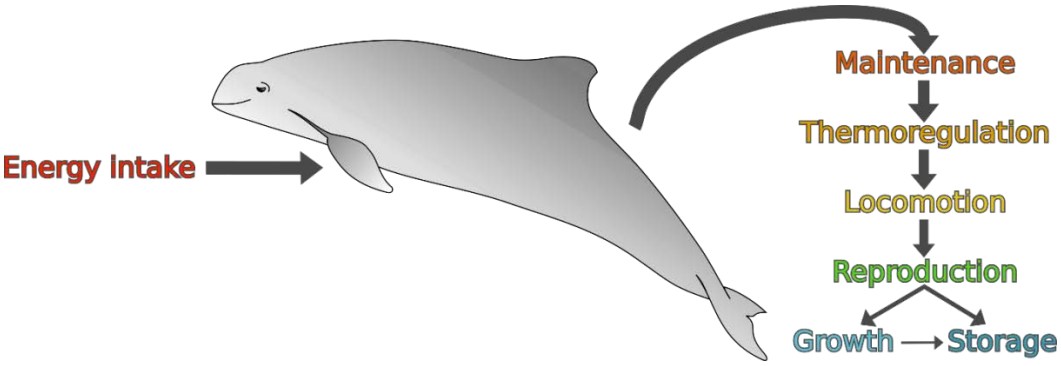

Figure 2.4. Key processes underlying energy budget. Line order signifies order of allocation. Line weight depicts the usage of energy at each step.

2.7.2.3 Sub-submodels

2.7.2.3.1 Energy intake

Table 2.6. Parameters used in the energy intake sub-submodel.

Symbol	Value	Code	Description [units] (reference)

IR_{scaling}	0.0004	IR_Coef	Maximum ingestion rate [J 30min-1] (calibrated)
ϖ	10	satiation_C	Satiation constant [unitless] (calibrated)
AE	0.82	AE_Food	Assimilation efficiency of food [%] (Kriete 1994)
IR_2EA	1.1375×10^8	IR2EA	Conversion from ingested food to energy in joules (calibrated)

Table 2.7. Equations used in the energy intake sub-submodel.

Eqn#	Function [units]	Code	Symbol	Equation	Source
13	Potential ingestion rate in a timestep based on structural mass [food units 30min^{-1}]	IR_Struct_Mass	IR_{str}	$IR_{\text{scaling}} \times {m_{\text{str}}}^{0.75} \times IR_{T,\text{mod}}$	Brown et al. 2004 & modified by temperature
14	Ingestion rate temperature modifier [unitless]	IR_Temp_Mod	$IR_{T,\text{mod}}$	$\frac{1}{5} cos\left(\frac{1}{6.366} T_{\text{W}}[c]\right) + 1$	Based on results from Rojano-Doñate et al. 2018
15	Ingestion rate supplement for pregnant porps [food units 30min^{-1}]	preg_IR_Sup	IR_{Preg}	$\frac{M_{\text{P}}}{AE \times IR_2EA}$	-
16	Ingestion rate supplement for lactating porps [food units 30min^{-1}]	lact_IR_Sup	IR_{Lact}	$\frac{M_{\text{Lact}}}{AE \times IR_2EA}$	-
17	Total ingestion rate for a timestep [food units 30min^{-1}]	IR_Tick	IR_{ts}	$IR_{\text{St}} + IR_{\text{Preg}} + IR_{\text{Lact}}$	-
18	Ingestion rate [food units]	IR_Re	IR_{Rec}	$\sum_{ts} IR_{ts} \times ts$	-
19	Maximum storage level based on length [%]	max_SL	$SL_{\max}$	$-0.39635L + 1.02347$	calculated from IDW porpoise dataset
20	Estimator of how far over mean storage level [%]	over_Mean_SL	SL_{over}	$\frac{SL - SL_{\text{idl}}}{SL_{\max} - SL_{\text{idl}}}$	-
21	Ingestion rate modifier based on storage level [unitless]	IR_SL_Mod	$IR_{\text{SL,mod}}$	$e^{-\varpi \times SL_{\text{over}}}$	-
22	Assimilated energy [J]	e_Assim	EA	$IR_{\text{realized}} \times IR_2EA \times AE$	-
23	Calf maximum ingestion rate in a timestep based on structural mass [food 30min^{-1}]	IR_Struct_Mass_C	$IR_{\text{str,calf}}$	$IR_{\text{scaling}} \times {m_{\text{str,calf}}}^{0.75} \times IR_{T,\text{mod}}$	Brown et al. 2004 & modified by temperature
24	Calf assimilated energy [J]	e_Assim_Calf	EA_{calf}	$IR_{\text{realized,calf}} \times IR_2EA \times AE$	-

Once per timestep, when a porp visits a grid cell containing food, the food level in the grid cell (its utility; $U[c]$) drops corresponding to the rate of consumption of the porp (IR) ($U[c] = U[c] - (IR \times ts)$; where ts is the number of timesteps). At the end of each simulation day depleted patches update, i.e. replenish, their food levels after porps have moved and consumed food by increasing their food level logistically using the food growth rate, r_{U} (Table 2.2). The maximum food level of a grid cell can vary seasonally, and the season-specific estimates were conserved from Nabe-Nielsen et al. (2014).

Potential food intake rates, IR_{str}, (in food units 30min^{-1}) were estimated allometrically using structural body mass, m_{str}, (in food units) and an intake rate scaling coefficient, IR_{scaling}, and corrected based on seasonal variability in water temperature using the water

temperature dependent modifier, $IR_{T,\mathrm{mod}}$ (Eqn. 13). $IR_{T,\mathrm{mod}}$ is defined by a cosine function dependent on the water temperature, T_{W} (Eqn. 14) and follows the seasonality of ingestion rates reported for porpoises in Rojano-Doñate et al. (2018) & Kastelein et al. (2018). $IR_{T,\mathrm{mod}}$ is updated once per month, following the temperature map update.

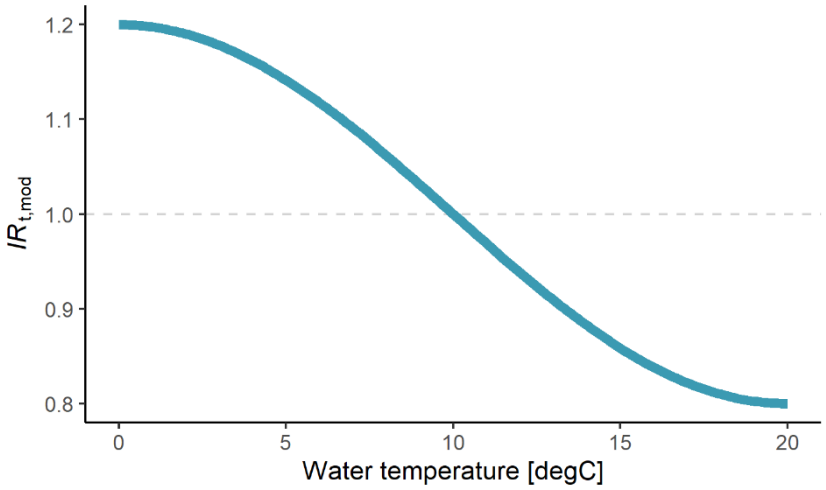

Figure 2.5. Relationship between water temperature, T_W, and the ingestion rate intake modifier, $IR_{T,mod}$.

Pregnant and lactating porps increase their ingestion rates to cover the energy used for pregnancy, IR_{Preg}, and lactation, IR_{Lact}, in the previous timestep (Eqns. 15 & 16). The total ingestion rate for the timestep, IR_{TS}, is then calculated as the sum of IR_{str}, IR_{Preg}, and IR_{Lact} (Eqn. 17).

If the food level of the grid cell (its utility; $U[c]$) occupied by porps is either zero or less than the amount of food they ingest during that timestep ($U[c] < IR_{ts}$), the amount of food ingested (IR) is reduced to the food level of the grid cell ($IR = \frac{U[c]}{ts}$). Porps keep track of their unmet ingestion needs ($IR_{ts} - (IR \times ts)$). These unmet needs can accrue through multiple timesteps ts (each 30 min) when insufficient food levels have been encountered and are stored in an ingestion record, IR_{Rec}, (Eqn. 18). In the following timestep, the potential realized ingestion rate is set to this record to accommodate for these periods, such that porps that haven't eaten in a longer period of time can ingest relatively more food once they encounter sufficient levels than porps that have recently encountered food.

Porps with storage exceeding ideal storage levels (SL_{idl}), as estimated using a linear fit of length and the average storage levels found for porpoises in McLellan et al. (2002) and adjusted seasonally using the temperature modifier, $IR_{T,\mathrm{mod}}$, reduce their intake rates exponentially as they reach their maximum storage level (as determined from the IDW porpoise dataset) (SL_{max}). This storage-level ingestion rate modifier, $IR_{\mathrm{SL,mod}}$, is determined using the porp's level of storage level excess, SL_{over} (calculated using Eqn. 20), and the unitless satiation constant, ϖ (Eqn. 21). The ingestion rate is then augmented by multiplying the realized ingestion rate, IR, by the storage level modifier, $IR_{\mathrm{SL,mod}}$.

After estimating IR, porps convert their ingested food to energy, in Joules, using the calibrated conversion constant IR_2EA and their assimilation efficiency EA (Eqn. 22), here 82% as the average value estimated for three fish eating killer whales in Kriete (1994). For

model simplicity, food was assumed to have a constant energy density regardless of location or season.

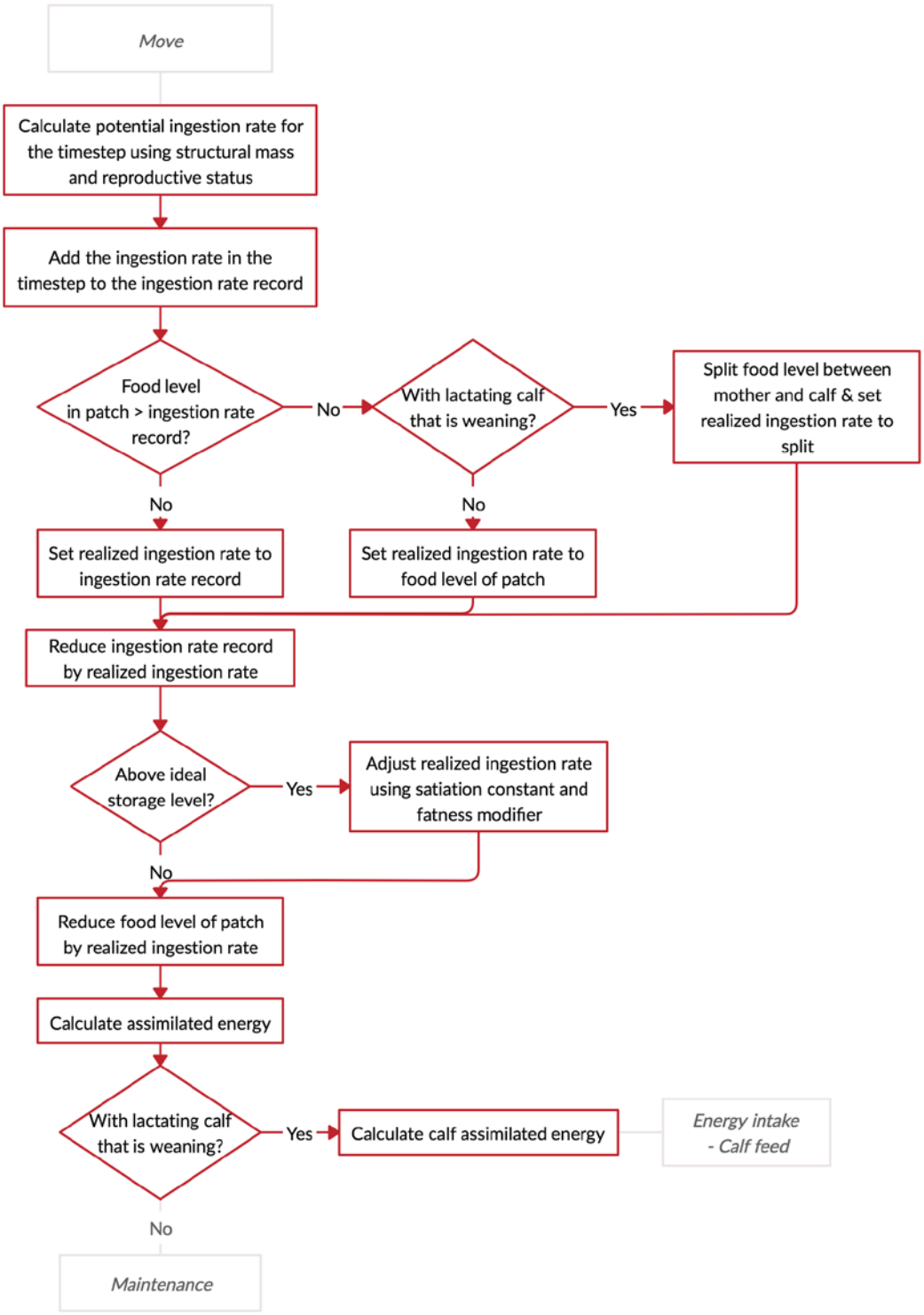

Figure 2.6. Summary of energy intake procedures. Diamond-shaped symbols indicate decisions made by porps, rectangles indicate calculations, and greyed out boxes represent other sub-submodels.

Calf feed: Porps with dependent calves that are weaning (i.e. ingesting any solid foods) calculate the ingestion rate of food from food patches for their calves based on their mass ($IR_{\mathrm{str,calf}}$) (Eqn. 23) each timestep and if insufficient food levels are encountered, calves

keep track of unmet needs following the same recording system as the mother, IR_{Rec}. This process is separate from the energy transferred via milk (milk energy is transferred in the *Lactation* sub-submodel) and relates only to solid foods being ingested from food patches by calves. When calves ingest food, it is converted to assimilated energy, EA_{calf}, using the same method as the mothers (Eqn. 24).

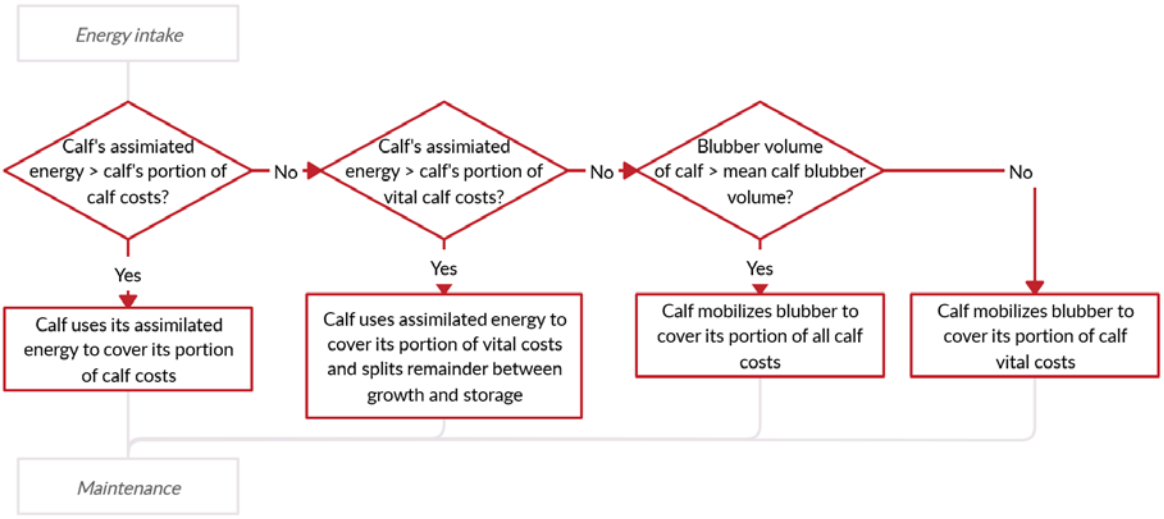

Figure 2.7. Summary of procedures related to feeding by dependent calves. Diamond-shaped symbols indicate decisions made by porps, rectangles indicate calculations, and greyed out boxes represent other sub-submodels.

2.7.2.3.2 Energy expenditure

Individual energy budgets were constructed for porps based on fundamental physical and physiological principles (Gallagher et al. 2018, Hind & Gurney 1997, Sibly et al. 2013, Brown et al. 2004). We are here using these principles, and the corresponding equations, as given sub-submodels taken from the literature, without further testing them or explaining their rationale in detail. The advantage of using them lies in the fact that the same sub-submodels can be used to any model energy budgets of cetaceans, so that our model can be re-used and adapted, if data for parameterization exists.

The total metabolic costs experienced by a porp at any time point (in J 30min^{-1}) are dependent on the animal's body size, condition, heat loss, activity level, and reproductive status. It can be represented by (Eqn. 25; Table 2.8):

Metabolic Costs = *Maintenance* + *Thermoregulation* + *Locomotion* (+ *Reproduction*) (+ *Growth*)

Table 2.8. Equation used to calculate total energy expenditure

Eqn#	Function [units]	Code	Symbol	Equation	Source
25	Total metabolic costs [J 30min^{-1}]	m_Tot	M	$M_{\mathrm{B}} + M_{\mathrm{T}} + M_{\mathrm{L}} + M_{\mathrm{P}} + M_{\mathrm{Lact}} + M_{\mathrm{G}}$	Gallagher et al. 2018

Basal maintenance rates, M_{B}, are dependent on the total body size of the animal. The cost of thermoregulation, M_{T}, and locomotion, M_{L}, also depend on body size in addition to the animal's activity level, body condition, and environmental parameters, e.g. salinity and temperature. Growth (M_{G}) and reproduction costs (pregnancy (M_{P}) and lactation (M_{Lac})

costs) only apply to growing and reproductively active individuals, respectively. Growth costs depend on the structural mass of the individual, while reproductive costs are influenced by the reproductive status and stage of the animal (see Table 2.5 for an overview of the state variables involved in determining each of these processes). After energy is assimilated from prey it can be applied to cover these costs in order of importance to survival and excess energy can be stored as blubber. If a deficit occurs, porps with blubber stores of adequate volume can mobilize blubber to cover costs, particularly vital costs, i.e. maintenance, thermoregulation, and locomotion.

Each of the modelled processes occur in two discrete steps. The first is the calculation of the total cost of the process (in J 30min^{-1}) (*Cost calculation*) and is presented below by using two tables for each process; one for the parameters related to the cost calculation (shaded) and one for the equations used. The second step is to allocate assimilated or mobilized energy to the various processes (*Allocation*). The algorithms related to allocation are visualized using a flow chart.

2.7.2.3.2.1 Maintenance

Table 2.9. Parameters used in the maintenance sub-submodel.

Symbol	Value	Code	Description [units] (reference)
B_0	N(11.15, 0.05)*	B0	Normalization constant [unitless] (calibrated)

*Normal distribution with mean and standard deviation

Table 2.10. Equations used in the maintenance sub-submodel.

Eqn#	Function [units]	Code	Symbol	Equation	Source
26	Maintenance costs [J 30min^{-1}]	m_BMR	M_{B}	$B_0 m^{0.75} \times 1800$	Kleiber 1975, Sibly et al. 2013

Cost calculation: The basal maintenance costs (M_{B}) for an animal are calculated using an allometric mass-scaling relationship (Eqn. 26) where B_0 represents the unitless normalization constant and m, the mass of the animal in kilograms. Using this relationship, the maintenance costs can be estimated, assuming it is not influenced by the animal's age, reproductive state, thermoregulatory status, or activity level, with only B_0 varying between species. The maintenance costs are multiplied by 1800 to convert the units from watts to joules per 30min timestep.

Allocation: After calculating maintenance costs, porps allocate energy to covering these costs (Fig. 2.8). First animals compare the total costs to the energy assimilated in that timestep (both in J). If the assimilated energy exceeds the total cost of maintenance, then costs are covered and the animal proceeds to the next process (*Thermoregulation*). If assimilated energy is insufficient, then the animal adds the assimilated energy to storage and compares the total stored energy to the costs of maintenance. If there is enough energy available in storage to cover maintenance costs, then stored energy is reduced by the costs of maintenance and the animal moves to the next process. If stored energy cannot cover the costs of maintenance, then the animal dies.

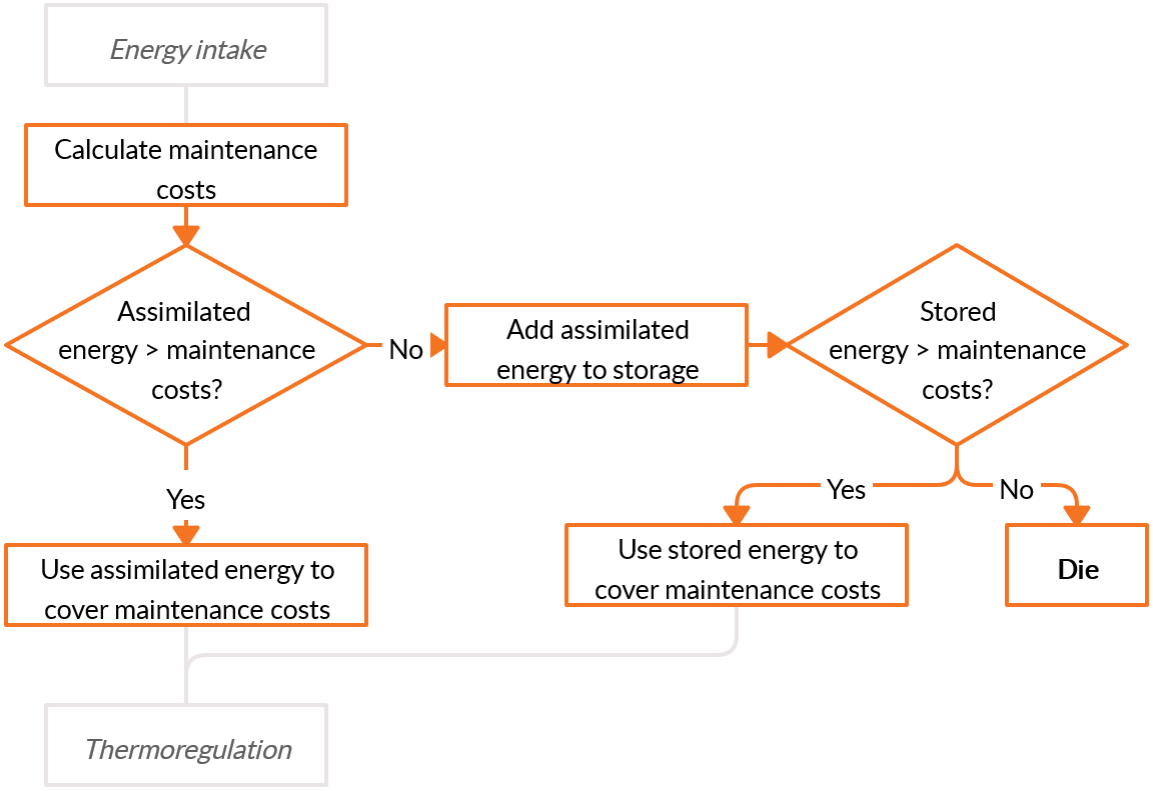

Figure 2.8. Process overview of energy allocation to maintenance costs. Diamond-shaped symbols indicate decisions made by porps, rectangles indicate calculations, and greyed out boxes represent other sub-submodels.

2.7.2.3.2.2 Thermoregulation

Table 2.11. Parameters used in the thermoregulation sub-submodel.

Symbol	Value	Code	Description [units] (reference)
T_C	N(36.7, 0.4)*	T_Core	Core temperature [°C] (Blanchet et al. 2008; pre-pregnancy)
k_B	N(0.10, 0.01)*	kB	Thermal conductivity of blood free blubber [W °C^{-1} m^{-1}] (Worthy & Edwards 1990)

*Normal distribution with mean and standard deviation

Cost calculation: The thermoregulatory costs of swimming porps, M_T, are determined using the morphometrics and swimming speed of porps and the location-specific temperature, salinity, and thermophysical properties of their environment. At the most basic level, M_T is represented as the difference between the total amount of energy needed to offset heat loss, Q_{CR}, and the minimum waste heat generated by the animal, Q_{CM}, (both in J 30min^{-1}) (Hind & Gurney 1997).

Table 2.12. Equations used in the thermoregulation sub-submodel.

Eqn#	Function [units]	Code	Symbol	Equation	Source
27	Locomotive waste heat from previous timestep [J 30min^{-1}]	m_Loco_Ineff_PTS	ε_L	$(1-\varepsilon_A)M_L$	Hind & Gurney 1997

28	Minimum heat generation rate [J 30min^{-1}]	min_Heat_Gen_Rate	Q_{CM}	$M_{\mathrm{B}} + \varepsilon_{\mathrm{L}}$	Hind & Gurney 1997
29	Total energy needed to offset heat loss [J 30min^{-1}]	heat_Gen_Rate_Real	Q_{CR}	$SA \times h_{\mathrm{CL}}(T_{\mathrm{C}} - T_{\mathrm{S}}) \times 1800$	Hind & Gurney 1997
30	The lower limit of the heat transfer coefficient [W °C^{-1}m^{-2}]	heat_Transfer_LL	h_{CL}	$\frac{k_B}{d_B}$	Hind & Gurney 1997
31	Realized temperature of the skin [°C]	T_SR	T_{S}	$\frac{11.4 \times k_{\mathrm{B}} \times L \times T_{\mathrm{mb}} + SA + T_{\mathrm{W}} \times h_{\mathrm{k}} \times \ln\left(\frac{m}{m_{\mathrm{st}}}\right)}{11.4 \times k_{\mathrm{B}} \times L + SA \times h_{\mathrm{k}} \times \ln\left(\frac{m}{m_{\mathrm{st}}}\right)}$	Ryg et al. 1993
32	Temperature of the blubber-muscle interface [°C]	T_MB	T_{mb}	$T_{\mathrm{C}} - ((T_{\mathrm{C}} - T_{\mathrm{W}}) \times 0.25)$	Estimated based on results of Worthy 1991 & George 2009
33	Forced convection scaling coefficient [W °C^{-1}m^{-2}]	fo_C_scaling_Coef	h_{k}	$0.036\left(\frac{k_{\mathrm{W}}}{L^{1/5}\nu^{4/5}}\right) Pr^{1/3} V^{4/5}$	Hind & Gurney 1997
34	Effective heat transfer coefficient [W °C^{-1}m^{-2}]	heat_Trans_Eff	h_{CE}	$\frac{\frac{Q_{\mathrm{CM}}}{1800}}{SA(T_{\mathrm{C}} - T_{\mathrm{S}})}$	Hind & Gurney 1997
35	Realized thermal costs [J 30min^{-1}]	m_Thermo	M_{T}	$\begin{cases} 0 & for\ h_{\mathrm{CE}} > h_{\mathrm{CL}} \\ Q_{\mathrm{CR}} - Q_{\mathrm{CM}} & otherwise \end{cases}$	Hind & Gurney 1997

Waste heat is produced during maintenance (M_{B}) and locomotive (M_{L}) processes. Heat generated as a consequence of maintenance can directly offset thermal needs, while waste heat associated with locomotion, ε_{L}, is generated based on the aerobic inefficiency (ε_{A}) (%) of the animal (see Locomotion section for details) (Eqn. 27; Table 2.12). The total waste heat (Q_{CM}) is then taken as the sum of these two processes (Eqn. 28).

The amount of energy needed to offset heat loss, Q_{CR}, is driven by the loss of heat generated in the core of the animal through its skin to the surroundings. As heat is being lost over the entire surface of the animal, Q_{CR} is dependent on the total surface area (SA) (in m^2), the minimum heat transfer coefficient of the blubber, h_{CL}, and the difference between the core, T_{C}, and velocity-specific actual skin temperature, T_{S} (in °C), of the animal (Eqn. 29). h_{CL} serves as the minimum estimate of heat transfer across the blubber layer as it is estimated as the ratio of the thermal conductivity of blood-free blubber (k_{B}) (in W °C^{-1}m^{-1}) over the blubber layer depth (d_{B}) (in m) (Eqn. 30). This assumes that marine mammals experiencing thermal stress adjust their peripheral blood flow to minimize heat loss (Hind & Gurney 1997). Q_{CR} is converted from watts to joules per 30min by multiplying by 1800. While the core temperature, T_{C}, and the blubber thermal conductivity, k_{B}, are literature-derived stochastic variables and the surface area, SA, and blubber depth, d_{B}, of animals can be calculated from their morphometrics and body condition, the skin temperature of swimming marine mammals, T_{S}, depends on factors related to the morphometrics and swimming speed of the animal and the current state of its environment.

Following the calculation of skin temperature due to convective heat loss in Ryg et al. (1993), the variables driving the realized skin temperature, T_{S}, of marine mammals are animal length (L) (in m), the temperature of the muscle-blubber interface (T_{mb}) (in °C), surface area (SA) (in m^2), the temperature of the water (T_{W}) (in °C), the heat transfer scaling coefficient for forced convection (h_{k}) (in W $°C^{-1}m^{-2}$), total mass of the animal (m), and structural mass (m_{st}) (in kg) (Eqn. 31). Here we calculate the temperature of the muscle-blubber interface (T_{mb}) as 75% of the difference between the core, T_{C}, and water temperature, T_{W}, (Eqn. 32), assuming that the thermal gradient for porpoises resembles those reported for bowhead whales (George 2009) and seals (Worthy 1991). The velocity-dependency of T_{S} influences the calculation of the heat transfer scaling coefficient for forced convection (h_{k}). This coefficient (Eqn. 33) allows for the estimation of heat loss, and therefore skin temperature, during swimming. It depends on the swimming speed (V) (in m s^{-1}) and length (L) (in m) of the animal as well as the thermophysical parameters determining heat conductivity in water: water conductivity (in W C^{-1} m^{-1}), k_{W}, kinematic viscosity (in m^2 s^{-1}), ν, and the Prandtl number (unitless), Pr. Once the realized skin temperature is calculated, Q_{CR} can be determined for animals of any size and body condition in their current environment.

During periods when the waste heat generated by an animal, Q_{CM}, results in an effective heat transfer across the body surface and h_{CE}, (calculated using Eqn. 34) greater than that of the minimum heat transfer coefficient (h_{CL}), the animal is assumed to be offloading excess heat to the environment. In that case no additional heat needs to be produced by the animal and the total cost of thermoregulation is set to zero. When h_{CE} is determined to be less than h_{CL} the animal loses more heat to the environment than it is producing and the total cost of thermoregulation is calculated as the difference between Q_{CR}, total energy needed to offset heat loss, and Q_{CM}, the waste heat generated by maintenance and locomotion (Hind & Gurney 1997) (Eqn. 35).

Cone specific calculations:
While blubber is used to insulate the body against heat loss, it is not distributed evenly across the body's surface (Koopman 1998) and when emaciated animals mobilize blubber, they do so in an uneven manner (Koopman et al. 2002). To account for these differences in blubber depth and their effect on heat loss, animals in the model are represented as a series of truncated cones with blubber depth (d_{B}) of animals measured at 9 points on the body and cones representing different lengths, as percentages of total body length (presented in detail in the Storage and Data Evaluation sections). For the thermoregulatory equations 30 & 33 the outputs are taken as the averages produced using the site-specific blubber depths ($d_{\mathrm{B,site}}$) and cone-specific lengths (L_{cone}). Blubber depths and cone lengths are updated once per day to account for fluctuations in blubber storage or mobilization throughout the simulation.

Allocation: After calculating thermoregulatory costs, porps allocate energy to covering thermoregulation (Fig. 2.9). First animals compare the total costs to the energy assimilated in that timestep (both in J). If the assimilated energy exceeds the total cost of thermoregulation, the unused energy can then be used to cover the costs of the next process (*Locomotion*). If assimilated energy is insufficient, then the animal adds the assimilated energy to storage and compares it the total to the costs of thermoregulation. If there is enough energy in storage to cover thermoregulatory costs, the stored energy is

reduced by the costs of thermoregulation and the animal moves to the next process. If stored energy cannot cover the costs of thermoregulation, the animal dies.

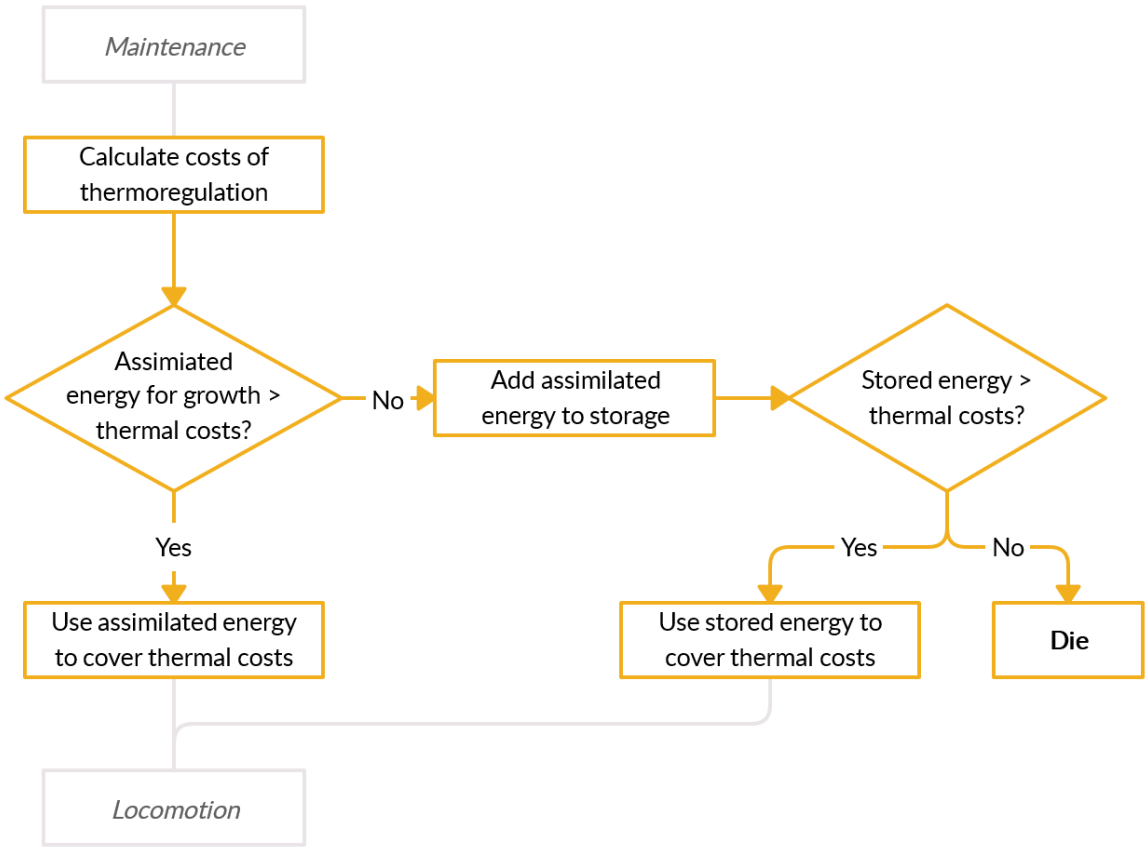

Figure 2.9. Process overview of energy allocation to thermal costs. Diamond-shaped symbols indicate decisions made by porps, rectangles indicate calculations, and greyed out boxes represent other sub-submodels.

2.7.2.3.2.3 Locomotion

Table 2.13. Parameters used in the locomotion sub-submodel.

Symbol	Value	Code	Description [units] (reference)
λ	N(0.25, 0.02)*	lambda	Ratio of active to passive drag [unitless] (calibrated)
ε_{P}	0.81	prop_Eff	Propeller efficiency [%] (Fish 1993)

*Normal distribution with mean and standard deviation

Table 2.14. Equations used in the locomotion sub-submodel.

Eqn#	Function [units]	Code	Symbol	Equation	Source
36	Aerobic efficiency [%]	aero_eff	ε_{A}	$0.1378 + 0.441\left(\frac{V}{4.2}\right)^{3} - 0.422\left(\frac{V}{4.2}\right)^{6}$	Hind & Gurney 1997
37	Reynold's number [unitless]	Re	Re	$\frac{V \times L}{\nu}$	Fish 1998
38	Drag coefficient [unitless]	drag_Coef	C_{D}	$10^{-0.1132 \times \log(Re) - 1.5358}$	Fit using results from Tanaka et al 2019

39	Cost of locomotion [J 30min^{-1}]	m_Loco	M_{L}	$\frac{\lambda \times \rho \times SA \times C_{\mathrm{D}} \times V^3}{2\varepsilon_{\mathrm{A}} \times \varepsilon_{\mathrm{P}}} \times 1800$	Hind & Gurney 1997

Cost calculation: The energy needed for an animal of a particular size to propel itself through the water at a specific swimming speed was calculated using the physics-based locomotive submodel in Hind & Gurney (1997). The total costs associated with movement depend on how efficiently stored/ingested energy is converted into movement. This comprises two aspects: (1) the propeller efficiency (ε_{P}) of the animal (%), defined as the ratio of thrust produced to total muscular work, and (2) the aerobic efficiency (ε_{A}) (%), which is defined as the efficiency of the body to transform chemical energy into muscular work (Hind and Gurney 1997). ε_{P} has been documented to be velocity-independent in marine mammals (Fish 1996, Hind and Gurney 1997), so this value was assumed to be constant. ε_{A} varies with work intensity such that the highest efficiencies are found at intermediate intensities (Gibbs and Gibson 1972) and for lift-based swimmers, such as cetaceans, it typically reaches approximately 25% (Fish 1996). The calculation of ε_{A} involves the ratio of the swimming speed of the animal (V) (in m s^{-1}) to the maximum swimming speed (Eqn. 36; Table 2.14). The equation is modified from Hind and Gurney 1997 to ensure a peak efficiency of 25% (Fish 1996) by adjusting the first constant and substituting the maximum swim speed with the reported value for porpoises of 4.2 m s^{-1} (Otani et al. 2001).

In addition to these efficiencies, the cost of locomotion depends on the velocity-specific drag experienced by the animal (Hind and Gurney 1997). Drag influences locomotive costs through the parameters λ, the ratio of the drag experienced by an actively swimming animal to the same animal being towed through the water at the same speed (unitless) (to account for drag reduction from active swimming), ρ, the water density (in kg m^{-3}), SA, the total surface area of the animal (in m^2), and C_{D}, the coefficient of drag (unitless). As the drag coefficient, C_{D}, of harbor porpoises is unknown, we calculated C_{D} using the relationship found between the drag coefficient and the Reynold's number (Re) in Tanaka et al. (2019) for the dolphin, *Lagenorhynchus obliquidens*. The Reynold's number, a unitless predictor of flow patterns, was estimated using the swimming velocity (V), length of the animal (L) (in m), and the kinematic viscosity of seawater (ν) (in m^2 s^{-1}) (Eqn. 37) and then used to calculate C_{D} using Eqn. 38.

The total metabolic cost of locomotion, M_{L} (in J 30min^{-1}), can then be calculated using Eqn. 39. Here M_{L} is converted from watts to joules per 30min by multiplying by 1800.

Allocation: After calculating locomotive costs, porps allocate energy to cover them (Fig. 2.10). First animals compare the total costs to the remaining assimilated energy (in J). If assimilated energy exceeds the total cost of locomotion, then the assimilated energy is reduced by the costs amount and the animal moves to the next process (*Reproduction*, *Growth*, or *Storage* depending on the state of the animal). If assimilated energy is not enough to cover locomotive costs, then the animal adds the assimilated energy to storage and compares the total to the costs of locomotion. If there is enough energy in storage to cover locomotive costs, the stored energy is reduced by the costs of locomotion and the animal proceeds to the next process. If stored energy cannot cover the costs of locomotion, the animal reduces costs and uses the remainder of stored energy to cover the process. As of now, this does not slow the animal down, but could do so easily in the future by influencing the fine-scale movements and reducing the swimming distance in a timestep.

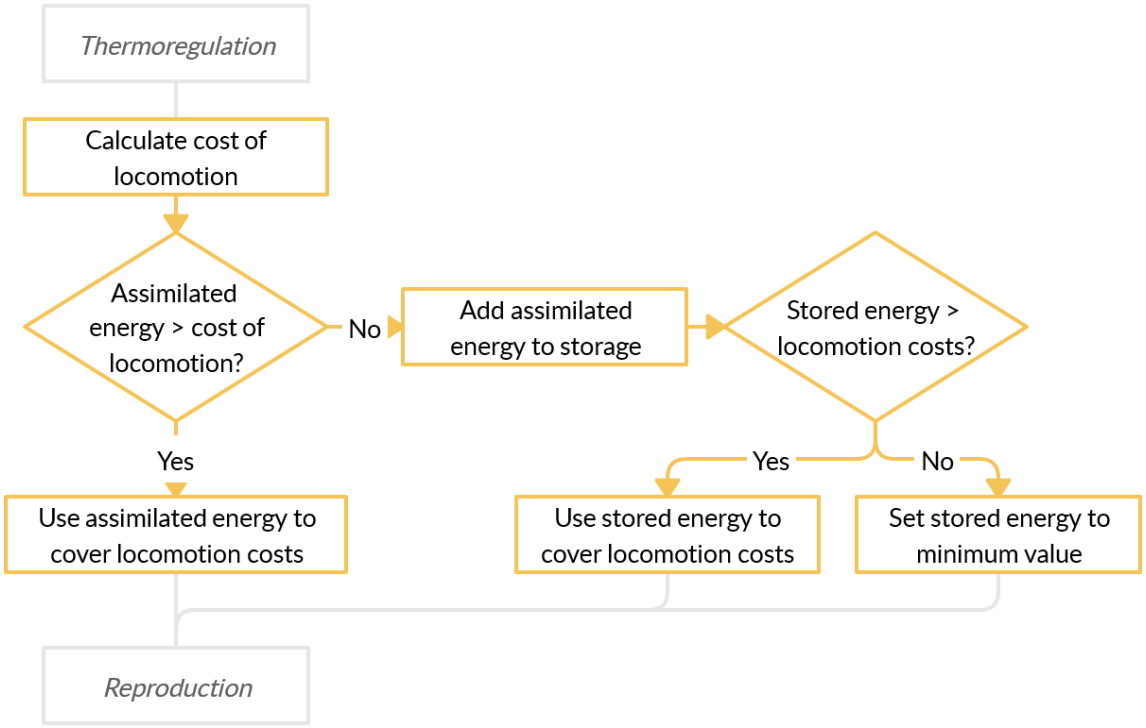

Figure 2.10. Process overview of energy allocation to locomotive costs. Diamond-shaped symbols indicate decisions made by porps, rectangles indicate calculations, and greyed out boxes represent other sub-submodels.

2.7.2.3.2.4 Reproduction

Table 2.15. Parameters used in the reproduction sub-submodel.

Symbol	Value	Code	Description [units] (reference)
fg	6.69×10^{-3}	fg	Fetal growth constant [unitless] (Read & Hohn 1995, Lockyer & Kinze 2003)
$\%_{f,lip}$	0.285	percent_Lip_F	Fetal body composition-Lipid [%] (McLellan et al. 2002, Lockyer 1995)
$\%_{f,lm}$	0.139	percent_LM_F	Fetal body composition-Lean mass [%] (McLellan et al. 2002, Lockyer 1991)
$m_{f,max}$	8	max_Mass_F	Maximum fetal mass [kg] (Lockyer and Kinze 2003)
$L_{\infty,m}$	112.9	lgth_M_Inf_M	Maximum length for male calves [cm] (calculated from IDW porpoise dataset)
$L_{0,m}$	68.1	lgth_M_0_M	Initial length for male calves [cm] (calculated from IDW porpoise dataset)
$L_{k,m}$	6.2	lgth_k_M	Length growth constant for male calves [cm] (calculated from IDW porpoise dataset)
$L_{\infty,f}$	116.3	lgth_M_Inf_F	Maximum length for female calves [cm] (calculated from IDW porpoise dataset)
$L_{0,m}$	89.2	lgth_M_0_F	Initial length for female calves [cm] (calculated from IDW porpoise dataset)
$L_{k,m}$	3.3	lgth_k_F	Length growth constant for female calves [cm] (calculated from IDW porpoise dataset)

$m_{\mathrm{str,c,\infty}}$	N(15.43, 0.59)*	m_Str_Inf	Maximum structural mass for calves [kg] (calculated from IDW porpoise dataset)
$m_{\mathrm{str,c,0}}$	N(4.99, 0.97)*	m_Str_0	Initial structural mass for calves [kg] (calculated from IDW porpoise dataset)
k_{c}	N(20.95, 4.07)*	m_Str_k	Structural mass growth constant for calves [kg yr^{-1}] (calculated from IDW porpoise dataset)
$\varepsilon_{\mathrm{Lac}}$	0.84	lact_Eff	Lactation efficiency [%] (Agricultural Research Council 1980, Prentice and Prentice 1988, Anderson and Fedak 1987, Rechsteiner et al. 2013)
t_{gest}	300	t_Gest	Gestation time [days] (Lockyer et al., 2003)
t_{nurs}	240	t_Nurs	Nursing time [days] (Lockyer et al., 2003; Lockyer and Kinze, 2003)

*Normal distribution with mean and standard deviation

Pregnancy:
Cost calculation: If a pregnant porp's body condition does not drop below critical levels before 300 days after impregnation (t_{gest}) it gives birth and begins to nurse its calf (on approximately day 182 of the simulation year). The energy required during pregnancy (M_{P}) is approximated by the summation of the energetic cost of fetal tissue investment (T_{f}) (in J 30min^{-1}) and the metabolic cost of gestation (Q_{G}) (in J 30min^{-1}), which covers maintenance of reproductive tissues such as the placenta (Eqn. 40; Table 2.16).

To estimate T_{f}, it was necessary to first establish fetal growth rates in porpoises. To do so fetal masses (m_{f}) (in kg) were assessed up to the maximum length ($L_{\mathrm{f,max}}$) (in cm) using the weight-length regression found for fetal porpoises from the IDW in Lockyer & Kinze (2003) ($m_{\mathrm{f}} = 0.05 \times L_{\mathrm{f}}{}^{2.72 \pm 0.06}$) (n = 124). Assuming a linear increase in body length with pregnancy time, as in Read & Hohn (1995), the fetal growth constant (fg) was determined by fitting the fetal mass to days since conception (ds_{mating}) using a cubic function ($m_{\mathrm{f}} = \left(fg \times ds_{\mathrm{mating}}\right)^3$) (Boult et al. 2018). Using fg and the fetal mass, m_{f}, the change in fetal mass (Δm_{f}) can be determined for porps in a timestep (Eqn. 41). This change in mass is then converted to fetal tissue investment costs using parameters related to fetal body lipid and lean mass composition ($\%_{\mathrm{f,lip}}$ & $\%_{\mathrm{f,lm}}$, respectively), tissue energy densities (ED), and deposition efficiencies (DE) of lipid ($_{\mathrm{lip}}$) and protein ($_{\mathrm{pro}}$) (Eqn. 42). Fetal and female masses are tracked separately for use in other sub-submodels, excluding the calculation of the surface area for pregnant females to include the added surface area attributed to pregnancy. Here the total mass of the female is regarded as the sum of the female mass and twice the fetal mass, this is based on Blanchet et al. (2008) where the final mass of a pregnant female porpoise before delivering was approximately twice the average neonatal mass of porpoise calves (Lockyer & Kinze 2003). This additional mass is likely attributed to additional reproductive tissues, such as the placenta and amniotic fluid.

Heat of gestation, Q_G, (in J 30min^{-1}) is calculated using Brody's (1968) mass-based relationship and the maximum fetal mass ($m_{\mathrm{f,max}}$) converted to joules (using 4184 kCal J^{-1}) for the entire pregnancy period and then divided by the total number of timesteps in the pregnancy period (14400), resulting in the calculation of Q_G in J 30min^{-1} (Eqn. 43).

Table 2.16. Equations used in the reproduction sub-submodel.

Eqn#	Function [units]	Code	Symbol	Equation	Source
			Pregnancy		

Allocation: After calculating pregnancy costs, porps allocate energy to covering pregnancy (Fig. 2.11). First animals compare the total costs to the remaining assimilated energy (in J). If assimilated energy exceeds the total cost of pregnancy, then the assimilated energy is reduced by the costs amount, the fetus grows, and the animal moves to the next process (*Lactation* or *Growth* and *Storage* depending on the state of the animal). If assimilated energy is not enough to cover pregnancy costs, then the animal adds any assimilated energy to storage and compares the total to the costs of pregnancy. If there is enough energy in storage to cover pregnancy costs without falling below the reproductive minimum, the stored energy is reduced by the costs of pregnancy and the animal moves to the next process. If stored energy is not enough to cover pregnancy costs, then the animal aborts the fetus and proceeds to the next process.

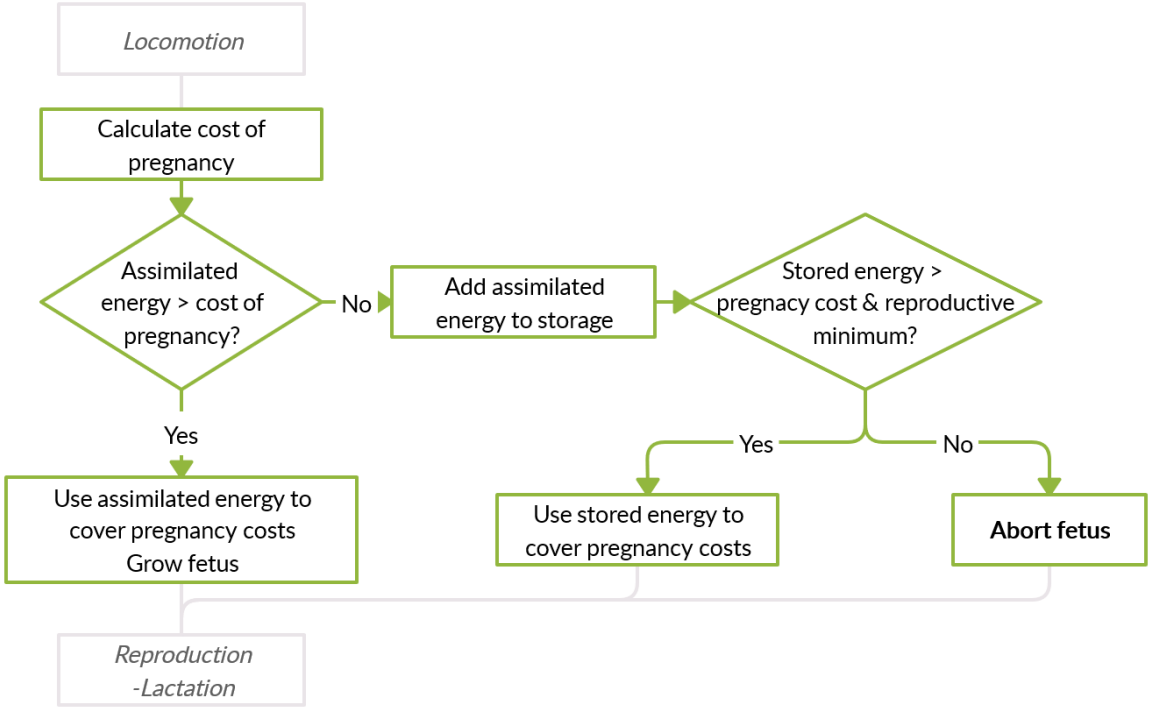

Figure 2.11. Process overview of energy allocation to pregnancy costs. Diamond-shaped symbols indicate decisions made by porps, rectangles indicate calculations, and greyed out boxes represent other sub-submodels.

40	Total cost of pregnancy [J 30min^{-1}]	m_Preg	M_{P}	$T_{\mathrm{f}} + Q_{\mathrm{G}}$	-
41	Fetal growth rate [kg 30min^{-1}]	max_Grow_F	Δm_{f}	$\frac{3fg^3 \times \left(\frac{{m_f}^{\frac{1}{3}}}{fg}\right)^2}{48}$	Boult et al. 2018
42	Fetal tissue investment [J 30min^{-1}]	e_Growth_F	T_{f}	$\frac{\Delta m_{\mathrm{f}} \times \%_{\mathrm{f,lip}} \times ED_{\mathrm{lip}}}{DE_{\mathrm{lip}}} + \frac{\Delta m_{\mathrm{f}} \times \%_{\mathrm{f,lm}} \times ED_{\mathrm{pro}}}{DE_{\mathrm{pro}}}$	Based on Boult et al. 2018
43	Heat of gestation [J 30min^{-1}]	e_Heat_Gest	Q_{G}	$\frac{4400\, {m_{\mathrm{max,f}}}^{1.2} 4184}{14400}$	Brody 1968
			Lactation		
44	Calf maintenance costs [J 30min^{-1}]	m_BMR_Calf	$M_{\mathrm{B,calf}}$	${B_0 m_{\mathrm{calf}}}^{0.75} \times 1800$	Kleiber 1975
45	Calf length based on age [m]	lgth_calf	L_{calf}	Calculated as in growth section (Eqn. 57) but using calf specific length parameters	Gol'din et al. 2004
46	Forced convection scaling coefficient of calf [W °C^{-1}m^{-2}]	fo_C_Scal_Coef_C	$h_{\mathrm{k,calf}}$	Calculated as in thermoregulation section (Eqn. 33) but using L_{calf}	Hind & Gurney 1997
47	Calf storage level [%]	storage_Level_Calf	SL_{calf}	$\frac{m_{\mathrm{calf}} - m_{\mathrm{str,calf}}}{m_{\mathrm{calf}}}$	-
48	Average blubber depth of the calf [m]	dB_calf	$d_{\mathrm{B,calf,avg}}$	$6.2154\, SL_{\mathrm{calf}} + 0.2512$	calculated from IDW porpoise dataset
49	Calf costs of thermoregulation [J 30min^{-1}]	m_Thermo_calf	$M_{\mathrm{T,calf}}$	Calculated as in thermoregulation section (Eqns. 27-32 & 33-35) using $h_{\mathrm{k,calf}}$	-
50	Calf costs of growth [J 30min^{-1}]	m_Growth_Calf	$M_{\mathrm{G,calf}}$	Calculated as in growth section but using calf specific growth parameters	-
51	Calf costs of blubber maintenance [J 30min^{-1}]	m_Blub_Calf	$M_{\mathrm{bl,calf}}$	$\frac{\left(V_{\mathrm{bl,calf}} - V_{\mathrm{bl,c,idl}}\right) \times \rho_{\mathrm{lip}} \times \%_{\mathrm{bl,lip}} \times ED_{\mathrm{lip}}}{DE_{\mathrm{lip}}}$	-
52	Total cost of lactation [J 30min^{-1}]	m_Calf	M_{Lact}	$\frac{M_{\mathrm{B,calf}} + M_{\mathrm{T,calf}} + M_{\mathrm{G,calf}} + M_{\mathrm{bl,calf}}}{\varepsilon_{\mathrm{Lac}}} \times w_{\mathrm{sf}}$	-

Lactation: Under ideal conditions the lactation period would last for 240 days (t_{nurs}) (Lockyer et al. 2003, Lockyer and Kinze 2003), ending on approximately simulation day 60, but under times of nutritional stress porps can choose to no longer allocate energy to lactation, potentially causing calf mortality. The cost of lactation (M_{Lac}) depends on several factors including the size and dependency level of the calf. As harbor porpoises have been noted to begin weaning their calves early into their lactation period (around 3mo) (Oftedal 1997, Camphuysen and Krop 2011), calves are considered to be 100% dependent up to that point and then dependency is decreased linearly to 0% by the end of the lactation period (as in Gallagher et al. 2018). The cost of lactation is determined by estimating the maintenance

(Eqn. 44), thermodynamic (Eqns. 45-49), growth (Eqn. 50), and the cost of building a sufficient blubber layer for the growing calf (Eqn. 51) using the same methods as for an adult porp and adjusting by a lactation efficiency ($\varepsilon_{\mathrm{Lac}}$) (Eqn. 52) (Table 2.16). For the thermodynamic calculations the calf-specific parameters $h_{\mathrm{k,calf}}$ & $d_{\mathrm{B,calf,avg}}$ were used as inputs in the thermal submodel and, as we assumed calf locomotive costs to be minimal due to echelon swimming, the minimum heat generation rate, Q_{CM}, was set to the basal metabolic costs of the calf, $M_{\mathrm{B,calf}}$.

Allocation: When female porps allocate energy to lactation, we assume that they first attempt to cover costs using the assimilated energy available for reproduction in a timestep. This is supported by observations of harbor porpoises primarily depending on increasing food intake, rather than blubber, to support the costs of lactation (Koopman et al. 1998, McLellan et al 2002). Under periods of low energy intake (when assimilated energy is not enough to cover lactation costs), we assume that female porps first check if their storage levels are of sufficient status, here represented by the mean blubber percentage found for lactating female porpoises in McLellan et al. (2002) (23.5% of body mass), and if their storage level exceeds this mean value, they mobilize blubber to cover all calf costs. If their storage level falls below the mean, to conserve blubber when body condition is low, they then check their storage levels against a reproductive minimum, here taken as the 10% of body mass (as in Beltran et al. 2017). If their storage level is greater than the minimum, but below the mean, porps allocate energy to cover only vital costs of the calf (i.e. maintenance and thermoregulation). If assimilated energy is greater than needed to cover vital costs, but storage level is below the mean, then porps will cover calf vital costs using the assimilated energy and partially cover growth and blubber costs using the remainder. If the female's blubber percentage falls below the reproductive minimum, then the calf must cover its own vital costs using its blubber layer or by foraging (if over 3mo). In this case, any energy assimilated by the female that would have be allocated to reproduction is then directed to storage. See Fig. 2.12 for a visual of this process.

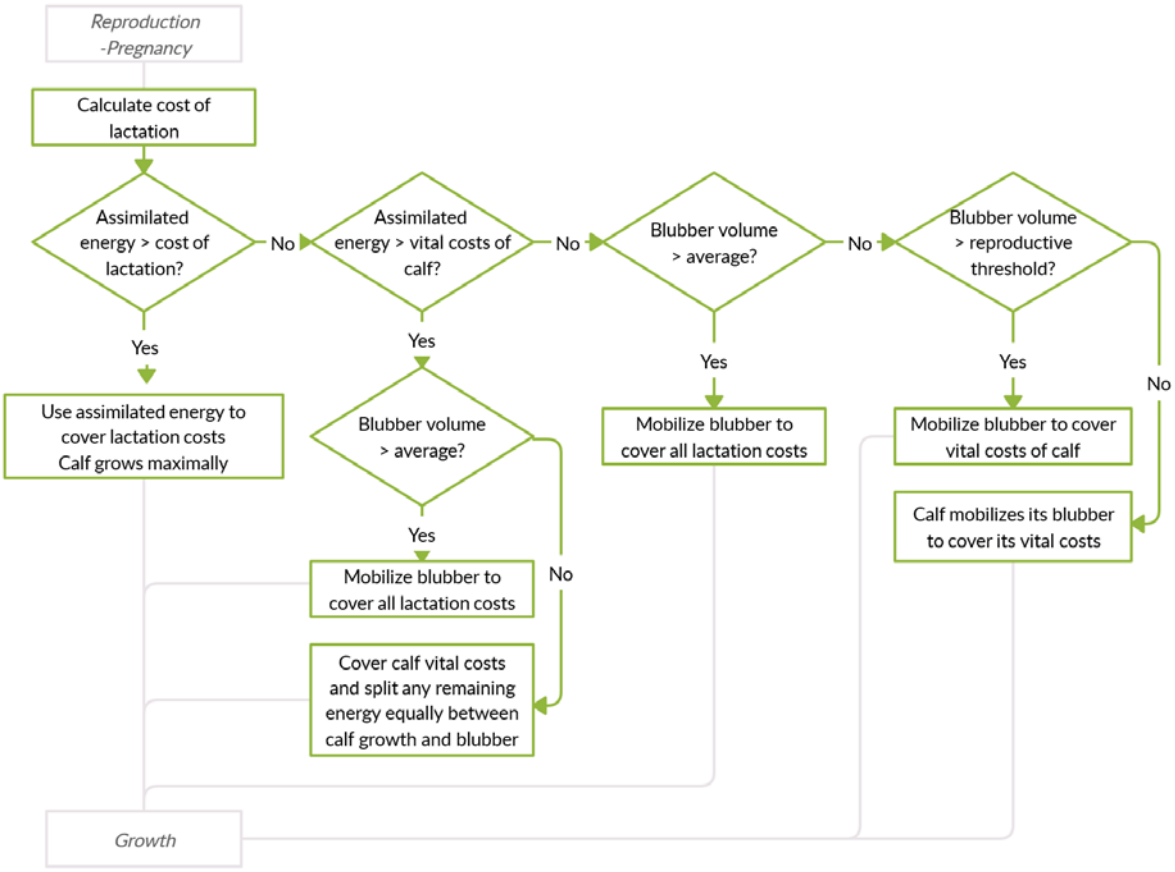

Figure 2.12. Process overview of energy allocation to lactation costs. Diamond-shaped symbols indicate decisions made by porps, rectangles indicate calculations, and greyed out boxes represent other sub-submodels.

2.7.2.3.2.5 Growth

Table 2.17. Parameters used in the growth sub-submodel.

Symbol	Value	Code	Description [units] (reference)
$\%_{\mathrm{lip}}$	U(1.74, 4.02)**	sm_Percent_Lip	Percent structural mass that is lipid [%] (Lockyer 1991)
$\%_{\mathrm{pro}}$	U(0.2543, 0.2715)**	sm_Percent_Pro	Percent structural mass that is protein [%] (Lockyer 1991)
ED_{lip}	39.5	ed_Lip	Lipid energy density [MJ kg-1] (Brody 1968, Blaxter 1989)
ED_{pro}	23.6	ed_Pro	Protein energy density [MJ kg-1] (Brody 1968)
DE_{lip}	U(0.74, 0.9)**	de_Lip	Deposition efficiency of lipid [%] (Malavear 2002, Pullar & Webster 1977)
DE_{pro}	U(0.43, 0.56)**	de_Pro	Deposition efficiency of protein [%] (Malavear 2002, Pullar & Webster 1977)
$m_{\mathrm{str},\infty}$	N(46.68, 3.86)*	m_str_inf	Maximum structural mass [kg] (calculated from IDW porpoise dataset)
L_{∞}	N(158.12, 4.68)*	lgth_M_inf	Maximum length [cm] (calculated from IDW porpoise dataset)

L_0	N(94.82, 1.69)*	lgth_M_0	Initial length [cm] (calculated from IDW porpoise dataset)
L_k	N(0.41, 0.06)*	lgth_k	Length growth constant [cm] (calculated from IDW porpoise dataset)

*Normal distribution with mean and standard deviation
**Uniform distribution with minimum and maximum values

Table 2.18. Equations used in the growth sub-submodel.

Eqn#	Function [units]	Code	Symbol	Equation	Source
53	Maximum growth rate [kg 30min^{-1}]	max_Grow	$\Delta m_{\mathrm{str,max}}$	$\frac{k}{17280}\left(m_{\mathrm{str},\infty}{}^{1/3} m_{\mathrm{str}}{}^{2/3} - m_{\mathrm{str}}\right)$	Sibly et al. 2013
54	Cost of maximal growth [J 30min^{-1}]	m_Growth	$M_{\mathrm{G,max}}$	$\Delta m_{\mathrm{str,max}}\left(ED_{\mathrm{lm}} + \left(ED_{\mathrm{lm}}(1 - DE_{\mathrm{lm}})\right)\right)$	Boult et al. 2018
55	Energy density of lean mass [J kg^{-1}]	ed_LM	ED_{lm}	$\left(\%_{\mathrm{pro}} \times ED_{\mathrm{pro}}\right) + \left(\%_{\mathrm{lip}} \times ED_{\mathrm{lip}}\right)$	-
56	Deposition efficiency of lean mass [%]	de_LM	DE_{lm}	$\frac{\left(\%_{\mathrm{pro}} \times DE_{\mathrm{pro}}\right) + \left(\%_{\mathrm{lip}} \times DE_{\mathrm{lip}}\right)}{\%_{\mathrm{pro}} + \%_{\mathrm{lip}}}$	-
57	Realized growth costs [J 30min^{-1}]	m_Growth	M_{G}	$\begin{cases} M_{\mathrm{G,max}} & for\ AE_{\mathrm{G}} \geq M_{\mathrm{G,max}} \\ \frac{AE_{\mathrm{G}}}{ED_{\mathrm{lm}}} \times DE_{\mathrm{lm}} & otherwise \end{cases}$	Boult et al. 2018
58	Length based on age [m]	lgth	L	$L_\infty e^{\left(ln\left(\frac{L_0}{L_\infty}\right)\left(-e^{-L_k \times age}\right)\right)}$	Gol'din et al. 2004

Calculate costs: If available energy remains after allocation to maintenance, thermoregulation, locomotion, and, for reproductively active individuals, reproduction, porps divide this energy into two equal portions to allocate to growth and storage. The energy available for growth is used for generating structural mass. We defined structural mass as the difference between total mass and blubber stores. Following the derived von Bertalanffy growth curves determined for calves (<0.9 yr old) and adult porpoises from data on porpoises in the IDW (see TRACE Section 3.2 for a description of the growth curves), maximum growth rates ($\Delta m_{\mathrm{str,max}}$) (kg 30min^{-1}) can then be calculated for porps based on their current and maximal structural masses (Eqn. 53; Table 2.18).

The energy needed for maximal growth ($M_{\mathrm{G,max}}$) is then calculated by converting $\Delta m_{\mathrm{str,max}}$, into tissue growth using the energy density, ED_{lm}, and deposition efficiency, DE_{lm}, of lean mass (Eqn. 54); where ED_{lm}, in J kg^{-1}, is determined using the percent composition (%) and energy densities (ED) of lean mass lipid ($_{\mathrm{lip}}$) and protein ($_{\mathrm{pro}}$) (Eqn. 55), and , DE_{lm} is taken as the percent-weighted average of the deposition efficiencies (DE) of lean mass lipid ($_{\mathrm{lip}}$) and protein ($_{\mathrm{pro}}$) (Eqn. 56).

If insufficient energy is available to support maximum growth ($AE_{\mathrm{G}} \geq M_{\mathrm{G,max}}$), the growth rate is reduced accordingly (Eqn. 57).

Porpoise length depends on the age of animals in years (age) and was calculated using a Gompertz growth curve (Eqn. 58). The Gompertz parameters were derived from animals that were also used for modelling growth in structural mass (see TRACE Section 3.2 for details).

Allocation: After calculating growth costs, porps allocate energy to covering growth (Fig. 2.13). First animals compare the total costs to the available assimilated energy for growth (in J). If this exceeds the total cost of growth, then the assimilated energy is reduced equivalently, the animals grow maximally, and calculation of the next process (*Storage*) takes place. If assimilated energy for growth is not enough to cover growth costs, porps check if their storage levels are greater than the ideal storage level, SL_{idl}. If stores are found to be sufficient, then the animals pull additional energy from storage to cover growth costs and grow maximally. If not, they do not use stored energy, but instead reduce growth rates proportionately to the assimilated energy available for growth and grow suboptimally before proceeding to the next process.

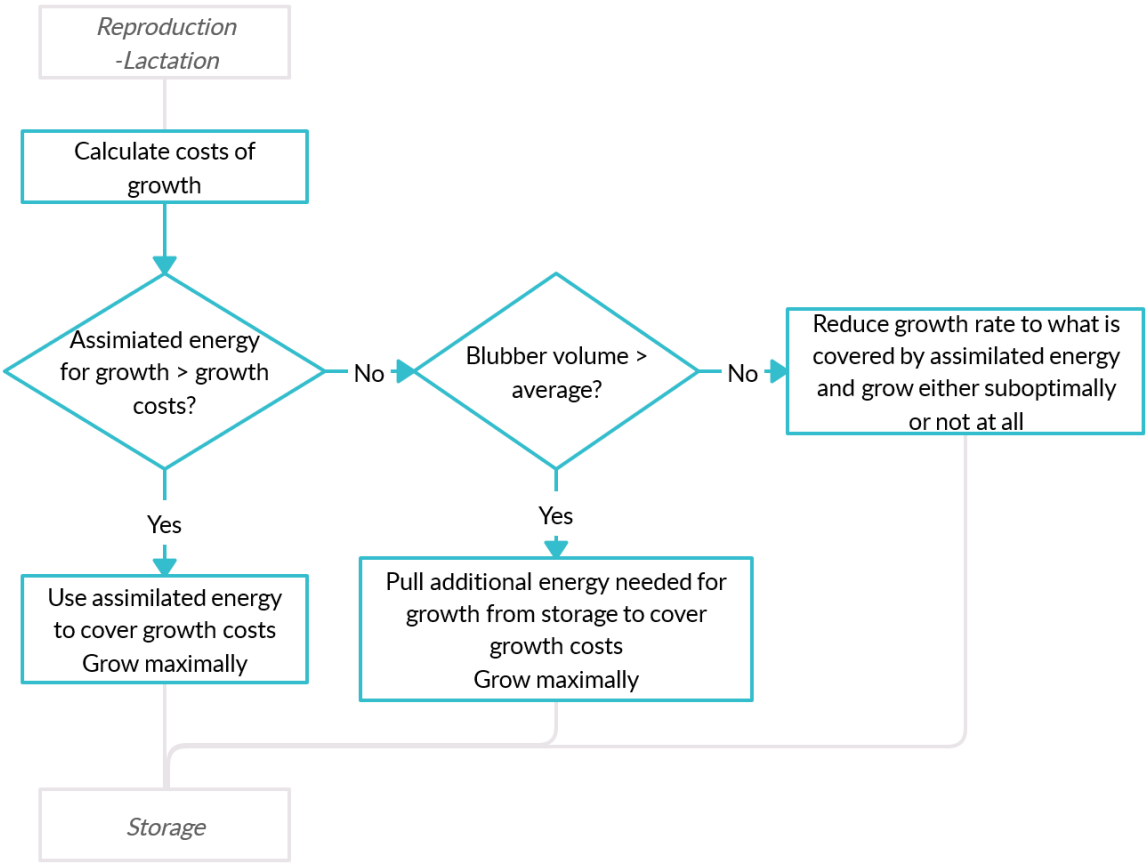

Figure 2.13. Process overview of energy allocation to growth costs. Diamond-shaped symbols indicate decisions made by porps, rectangles indicate calculations, and greyed out boxes represent other sub-submodels.

2.7.2.3.3 Storage

Table 2.19. Parameters used in the storage sub-submodel.

Symbol	Value	Code	Description [units] (reference)
$\%_{\mathrm{lip,bl}}$	N(0.816, 0.036)*	percent_Lip_Blub	Lipid percent in blubber [%] (Worthy & Edwards 1990)
ρ_{bl}	0.00092	dens_Blub	Blubber density [kg cm-3] (Parry 1949; adjusted for water content)

Site specific blubber depth slope: $q_{\mathrm{bl,X}}$ [unitless] (IDW porpoise dataset)			
Symbol	Value	Code	Description [units] (reference)
$q_{\mathrm{bl,AxD}}$	N(31.35, 13.46)*	q_bl_AxD	Dorsal axillary site
$q_{\mathrm{bl,AxL}}$	N(-23.86, 11.53)*	q_bl_AxL	Lateral axillary site
$q_{\mathrm{bl,AxC}}$	N(-45.16, 14.84)*	q_bl_AxV	Ventral axillary site
$q_{\mathrm{bl,CrD}}$	N(47.36, 13.80)*	q_bl_CrD	Dorsal cranial insertion of the dorsal fin site
$q_{\mathrm{bl,CrL}}$	N(9.8, 10.21)*	q_bl_CrL	Lateral cranial insertion of the dorsal fin site
$q_{\mathrm{bl,CrV}}$	N(-29.33, 14.27)*	q_bl_CrV	Ventral cranial insertion of the dorsal fin site
$q_{\mathrm{bl,CaD}}$	N(-14.62, 16.12)*	q_bl_CaD	Dorsal caudal insertion of the dorsal fin site
$q_{\mathrm{bl,CaL}}$	N(16.39, 12.87)*	q_bl_CaL	Lateral caudal insertion of the dorsal fin site
$q_{\mathrm{bl,CaV}}$	N(13.56, 14.36)*	q_bl_CaV	Ventral caudal insertion of the dorsal fin site
Site specific blubber depth intercept: $b_{\mathrm{bl,X}}$ [unitless] (IDW porpoise dataset)			
Symbol	Value	Code	Description [units] (reference)
$b_{\mathrm{bl,AxD}}$	N(1.42, 0.05)*	b_bl_AxD	Dorsal axillary site
$b_{\mathrm{bl,AxL}}$	N(1.58, 0.04)*	b_bl_AxL	Lateral axillary site
$b_{\mathrm{bl,AxV}}$	N(1.76, 0.05)*	b_bl_AxV	Ventral axillary site
$b_{\mathrm{bl,CrD}}$	N(1.53, 0.05)*	b_bl_CrD	Dorsal cranial insertion of the dorsal fin site
$b_{\mathrm{bl,CrL}}$	N(1.51, 0.04)*	b_bl_CrL	Lateral cranial insertion of the dorsal fin site
$b_{\mathrm{bl,CrV}}$	N(1.66, 0.05)*	b_bl_CrV	Ventral cranial insertion of the dorsal fin site
$b_{\mathrm{bl,CaD}}$	N(1.68, 0.06)*	b_bl_CaD	Dorsal caudal insertion of the dorsal fin site
$b_{\mathrm{bl,CaL}}$	N(1.46, 0.05)*	b_bl_CaL	Lateral caudal insertion of the dorsal fin site
$b_{\mathrm{bl,CaV}}$	N(1.42, 0.05)*	b_bl_CaV	Ventral caudal insertion of the dorsal fin site

*Normal distribution with mean and standard deviation

Table 2.20. Equations used in the storage sub-submodel.

Eqn#	Function [units]	Code	Symbol	Equation	Source
59	Blubber volume change [cm^3]	ch_Blub	ΔV_{bl}	$\frac{\left(AE_{\mathrm{S}} \times DE_{\mathrm{lip}} \times \%_{\mathrm{lip,bl}}\right)}{ED_{\mathrm{lip}} \times \rho_{\mathrm{lip}}}$	-
60	Site specific blubber depth [cm]	dB_Site	$d_{\mathrm{B,site}}$	$\left(q_{\mathrm{bl,X}} \frac{SL}{100L} + b_{\mathrm{bl,X}}\right) d_{\mathrm{B,avg}}$	IDW porpoise dataset
61	Average blubber depth [cm]	average_dB	$d_{\mathrm{B,avg}}$	$\frac{V_{\mathrm{bl}}}{SA \times 10000}$	-

Storing energy: Any available energy for storage is stored as blubber. At the end of each time step available energy to allocate to storage (AE_{S}) is first converted to blubber volume (ΔV_{bl}) (in cm^3). The amount stored depends on percent lipid of the blubber ($\%_{\mathrm{lip,bl}}$), deposition efficiency (DE_{lip}), energy density (ED_{lip}), and density of lipid (ρ_{lip}) (in kg cm^{-3}) (Eqn. 59). This change in blubber volume ΔV_{bl} is then added to the current blubber volume of the animal to determine the total storage volume (V_{bl}; cm^3).

Mobilizing storage: Whenever a porp uses stored energy to cover metabolic costs, this energy must be mobilized from stored blubber. To do this, the same process as for storing energy is used, but here the energy deficit is used to calculate the reduction in blubber volume (ΔV_{bl}) (using Eqn. 59) and this change is subtracted from the total blubber volume of the animal (V_{bl}). This decrease in blubber volume occurs on demand as the porp covers necessary costs.

Estimating site-specific blubber depth: Once per day, animals update their site-specific blubber depth $d_{\mathrm{B,site}}$; in cm) for 9 body sites to reflect their current body size and condition. The blubber depth at each site is estimated using linear relationships established between the body-site specific blubber depth ($d_{\mathrm{B,site}}$) for each of the 9 body sites and the storage levels (SL; in %), body lengths (L; in m), and average blubber depth over the entire body ($d_{\mathrm{B,avg}}$; in cm) of porps (Eqn. 60). Here average blubber depth ($d_{\mathrm{B,avg}}$) was estimated by spreading the total blubber volume of the animal (V_{bl}; in m^3) over the body surface area (SA; in m^2) (Eqn. 61). The linear relationships were established using the gls function in the package 'nlme' (Pinheiro et al. 2019) in R Statistical Software v.3.6.0 (R Core Team 2019).

2.7.2.3.4 Life history

Table 2.21. Parameters used in the life history sub-submodel.

Symbol	Value	Code	Description [units] (reference)
h	0.67	pregnancy_Rate	Probability of becoming pregnant [%] (Sørensen & Kinze 1994)
β_{S}	11.5	x_Survival_Prob_Constant	Survival probability constant [unitless] (calibrated)

Table 2.22. Equations used in the life history sub-submodel.

Eqn#	Function [units]	Code	Symbol	Equation	Source
62	Yearly survival probability [%]	yearly_Surv_Prob	S_{y}	$1-\left(c_{\mathrm{MR}} \times e^{-\beta_{\mathrm{S}} \times SL}\right)$	Nabe-Nielsen et al. 2014
63	Mortality rate offset constant [unitless]	m_Mort_Prob_Const	c_{MR}	$10^{2.176e^{-2} \times \beta_{\mathrm{S}} - 3.875e^{-4}}$	-
64	Survival probability [%]	daily_Surv_Prob	S_{d}	$e^{\log(S_{\mathrm{y}})/360}$	Nabe-Nielsen et al. 2018

Pregnancy can occur during the mating period for random mature females of adequate body condition at a rate consistent with the average of the pregnancy rates reported for IDW porpoises using two different estimation methods (67%) (Sørensen & Kinze 1994). During the calving period, pregnant females give birth. During the weaning period, lactating females wean calves. The weaned calf then becomes a new, independent individual in the model and the adult female records the calf as successfully weaned. If a female is experiencing nutritional stress and she is either pregnant or lactating, the calf may die depending on the body condition of the female (if pregnant) or the calf (if lactating). The survival probability is checked once a day for all porps, including dependent calves.

Survival probability: The survival of animals is assumed to be linked to their level of stored energy, such that animals with lower storage levels have a higher probability of mortality. The yearly survival probability, S_{y}, (%) is calculated for both adults and dependent calves and is estimated using the survival probability constant, β_{S}, (unitless). β_{S} determines the relationship between the porp's storage level (SL) and its probability of surviving one year at that level (as in Nabe-Nielsen et al. 2014, 2018) (Eqn. 62; Table 2.22). The ensure that the point of 100% mortality occurs at the minimum storage level found in the porpoise dataset of 5%, the parameter c_{MR} is used to offset S_{y} based on the value of β_{S} (Eqn. 63). S_{y} is

converted to a daily probability of mortality, S_{d}, (Eqn. 64) and checked once per day by producing a random number between 0–1, ω, and comparing it to S_{d}. If $\omega > S_{\mathrm{d}}$, the animal dies of low storage levels.

Animals can also die if they reach their maximum age of 30 years. Once per day the age of porps is checked and if their age exceeds 30 years they die.

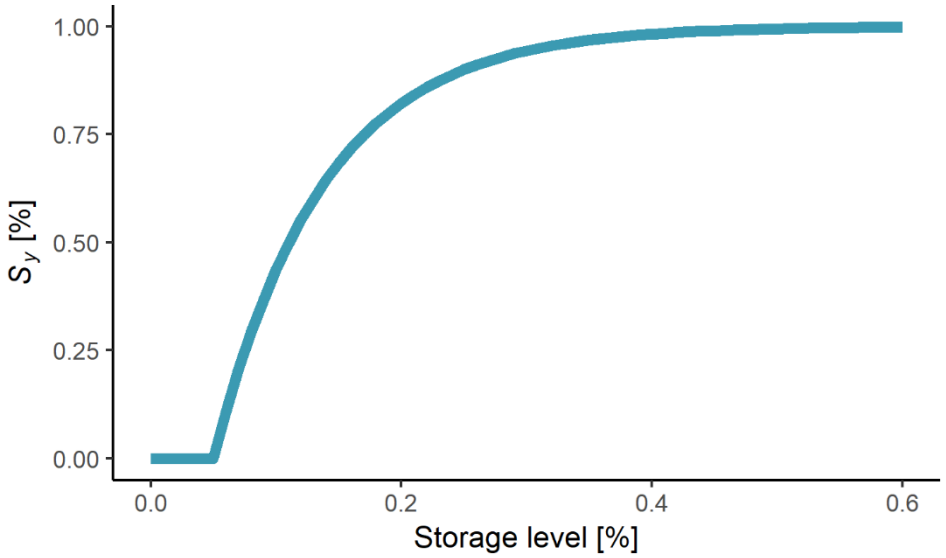

Figure 2.14. Relationship between storage level and yearly mortality for β_S = 11.5 (resulting c_{MR}= 1.78).

2.7.2.3.5 Update state variables

Table 2.23. Parameters used to update porp state variables.

Symbol	Value	Code	Description
SL_{min}	0.05	min_Blub_Perc	Minimum storage level [%] (IDW porpoise dataset)
SL_{R}	0.1	repro_Min_Blub_Perc	Reproductive storage level threshold [%] (Beltran et al. 2017)
$SL_{\mathrm{calf,idl}}$	0.375	calf_Idl_Blub_Perc	Calf ideal storage level [%] (McLellan et al. 2002)

At the end of each time step, after running energetic procedures, porps update their state variables. The total metabolic rates of animals (in J 30min^{-1}) are estimated by summing the costs of each of the expenditures experienced by the animal in that time step (Eq. 25; Table 2.8). The total weight of the animal is updated at this point by adding the structural mass (m_{str}; in kg) to blubber mass, represented as the total blubber volume (V_{bl}) converted to mass using the blubber density (ρ_{lip}) (Eqn. 65; Table 2.24). The storage level of the animal (SL; %) is then determined as the percentage of total body mass (m; in kg) comprised of blubber (Eqn. 66) and the surface area of the animal (SA; in m^2) is updated using total body mass (Eqn. 67). The mean storage level (SL_{mean}; %) based on size and water temperature is then updated for animals (Eqn. 68) and then the blubber volume mean ($V_{\mathrm{bl,mean}}$), minimum

Table 2.24. Equations used to update porp state variables.

Eqn#	Function [units]	Code	Symbol	Equation	Source
65	Mass [kg]	weight	m	$m_{\mathrm{str}} + (V_{\mathrm{bl}} \times \rho_{\mathrm{lip}})$	-
66	Storage level [%]	storage_Level	SL	$\frac{m - m_{\mathrm{str}}}{m}$	-
67	Surface area [m2]	surface_Area	SA	$0.093m^{0.57}$	Worthy and Edwards 1990
68	Mean storage level [%]	SL_Mean	SL_{mean}	$(-0.3059L + 0.7066)IR_{T,\mathrm{mod}}$	-
69	Mean blubber volume [cm^3]	v_Blub_Mean	$V_{\mathrm{bl,mean}}$	$\frac{m \times SL_{\mathrm{mean}}}{\rho_{\mathrm{lip}}}$	-
70	Minimum blubber volume [cm^3]	v_Blub_Min	$V_{\mathrm{bl,min}}$	$\frac{m \times SL_{\mathrm{min}}}{\rho_{\mathrm{lip}}}$	-
71	Reproductive blubber volume threshold [cm^3]	v_Blub_Repro	$V_{\mathrm{bl,R}}$	$\frac{m \times SL_{\mathrm{repro}}}{\rho_{\mathrm{lip}}}$	-
72	Available energy in storage [J]	e_Storage	E_{stor}	$(V_{\mathrm{bl}} - V_{\mathrm{bl,min}})\rho_{\mathrm{lip}} \times ED_{\mathrm{lip}}$	-
73	Reproductive energy threshold [J]	e_Repo_Min	$E_{\mathrm{R,min}}$	$(V_{\mathrm{bl,R}} - V_{\mathrm{bl,min}})\rho_{\mathrm{lip}} \times ED_{\mathrm{lip}}$	-
74	Calf mass [kg]	mass_C	m_{calf}	$m_{\mathrm{str,calf}} + (V_{\mathrm{bl,calf}} \times \rho_{\mathrm{lip}})$	-
75	Ideal calf blubber volume [cm^3]	v_Blub_Calf_Idl	$V_{\mathrm{bl,c,idl}}$	$\frac{m_{\mathrm{calf}} \times SL_{\mathrm{calf,idl}}}{\rho_{\mathrm{lip}}}$	-

($V_{\mathrm{bl,min}}$), and reproductive threshold ($V_{\mathrm{bl,R}}$) (in cm^3) are updated (Eqns. 69-71) using a minimum storage level (SL_{min}) of 0.05 and a storage level reproductive threshold (SL_{R}) of 0.10. The total amount of energy available in storage (E_{stor}; in J) is then calculated using the difference between V_{bl} & $V_{\mathrm{bl,min}}$, and the density (ρ_{lip}; kg cm^{-3}) and energy density of lipid (ED_{lip}; J kg^{-1}) (Eqn. 72). The reproductive threshold is then calculated in the same manner but using $V_{\mathrm{bl,R}}$ rather than $V_{\mathrm{bl,min}}$ (Eqn. 73). Lactating porps update the mass of their calves (m_{calf}; kg) using the calf structural mass ($m_{\mathrm{str,calf}}$; kg) and blubber volume ($V_{\mathrm{bl,calf}}$; cm^3) determined during the lactation procedure (Eqn. 74). Then using the ideal storage level for calves ($SL_{\mathrm{calf,idl}}$; %), the ideal calf blubber volume ($V_{\mathrm{bl,c,idl}}$; cm^3) is calculated (Eqn. 75).

References

Agricultural Research Council, 1980. *The Nutrient Requirements of Ruminant Livestock*. Slough, Berks.

Anderson, S.S. and Fedak, M.A., 1987. Grey seal, Halichoerus grypus, energetics: females invest more in male offspring. Journal of Zoology, 211(4), pp.667-679.

Barham, R.J., 2016. Omø South Nearshore A/S: Underwater noise. Orbicon A/S. Technical Report from Orbicon & Subacoustech Environmental Ltd No. OS-TR-003. URL: https://ens.dk/sites/ens.dk/files/Vindenergi/os-tr-003_underwater_noise.pdf

Beltran, R.S., Testa, J.W. and Burns, J.M., 2017. An agent-based bioenergetics model for predicting impacts of environmental change on a top marine predator, the Weddell seal. Ecological Modelling, 351, pp.36-50.

Blanchet, M., Nance, T., Ast, C., Wahlberg, M. and Acquarone, M., 2008. First case of a monitored pregnancy of a harbour porpoise (Phocoena phocoena) under human care. Aquatic Mammals, 34(1), p.9.

Blaxter, K., 1989. *Energy metabolism in animals and man*. CUP Archive.

Boult, V.L., Quaife, T., Fishlock, V., Moss, C.J., Lee, P.C. and Sibly, R.M., 2018. Individual-based modelling of elephant population dynamics using remote sensing to estimate food availability. Ecological modelling, 387, pp.187-195.

Brody, S. 1968. *Bioenergetics and growth*. Hafner Publishing Company Inc. New York, NY.

Brown, J.H., Gillooly, J.F., Allen, A.P., Savage, V.M. and West, G.B. 2004. Toward a metabolic theory of ecology. Ecology, 85, 1771–1789.

Camphuysen, C. J., and Krop, A. 2011. Maternal care, calf-training and site fidelity in a wild harbour porpoise in the North Sea. Lutra 54:123-126.

Edrén, S., Wisz, M.S., Teilmann, J., Dietz, R. and Söderkvist, J., 2010. Modelling spatial patterns in harbour porpoise satellite telemetry data using maximum entropy. Ecography, 33(4), pp.698-708.

Fish, F.E., 1993. Power output and propulsive efficiency of swimming bottlenose dolphins (Tursiops truncatus). Journal of Experimental Biology, 185(1), pp.179-193.

Fish, F.E. 1996. Transitions from drag-based to lift-based propulsion in mammalian swimming. American Zoologist, 36(6), pp.628-641.

Fish, F.E., 1998. Comparative kinematics and hydrodynamics of odontocete cetaceans: morphological and ecological correlates with swimming performance. Journal of Experimental Biology, 201(20), pp.2867-2877.

Gallagher, C.A., Stern, S.J. and Hines, E., 2018.The metabolic cost of swimming and reproduction in harbor porpoises (*Phocoena phocoena*) as predicted by a bioenergetic model. Marine Mammal Science. Doi: https://doi.org/10.1111/mms.12487

George, J., 2009. *Growth, morphology and energetics of bowhead whales, Balaena mysticetus*, University of Alaska Fairbanks, Fairbanks. PhD thesis. URL: http://hdl.handle.net/11122/9031

Gibbs, C.L. and Gibson, W.R., 1972. Energy production of rat soleus muscle. American Journal of Physiology-Legacy Content, 223(4), pp.864-871.

Gol'din, P. E. 2004. Growth and body size of the harbour porpoise, Phocoena phocoena (Cetacea, Phocoenidae), in the Sea of Azov and the Black Sea.

Hind, A.T. and Gurney, W.S., 1997. The metabolic cost of swimming in marine homeotherms. Journal of Experimental Biology, 200(3), pp.531-542.

Kastelein, R.A., Helder-Hoek, L. and Jennings, N., 2018. Seasonal changes in food consumption, respiration rate, and body condition of a male harbor porpoise (Phocoena phocoena). Aquatic Mammals, 44(1), pp.76-91.

Kleiber, M., 1975. *The fire of life: an introduction to animal energetics*. Rev. ed. Pub Krieger RE, Malabar, Florida.

Koopman, H.N., 1998. Topographical distribution of the blubber of harbor porpoises (Phocoena phocoena). Journal of Mammalogy, 79(1), pp.260-270.

Koopman, H.N., Pabst, D.A., Mclellan, W.A., Dillaman, R.M. and Read, A.J., 2002. Changes in blubber distribution and morphology associated with starvation in the harbor porpoise (Phocoena phocoena): evidence for regional differences in blubber structure and function. Physiological and Biochemical Zoology, 75(5), pp.498-512.

Kriete, B., 1994. *Bioenergetics in the killer whale, orcinus orca*, University of British Columbia, Vacncouver. PhD thesis. Doi: 10.14288/1.0088104

Kyhn, L.A., Wisniewska, D.M., Beedholm, K., Tougaard, J., Simon, M., Mosbech, A. and Madsen, P.T., 2019. Basin-wide contributions to the underwater soundscape by multiple seismic surveys with implications for marine mammals in Baffin Bay, Greenland. Marine pollution bulletin, 138, pp.474-490.

Lockyer, C., 1991. Body composition of the sperm whale, Physeter catodon, with special reference to the possible functions of fat depots. Marine Research Institute.

Lockyer, C. 1995. Investigation of aspects of the life history of the harbour porpoise, Phocoena phocoena, in British waters. Report of the International Whaling Commission, pp.189-199.

Lockyer, C., 2003. Harbour porpoises (Phocoena phocoena) in the North Atlantic: Biological parameters. NAMMCO Scientific Publications, 5, pp.71-89.

Lockyer, C. and Kinze, C., 2003. Status, ecology and life history of harbour porpoise (Phocoena phocoena), in Danish waters. NAMMCO Scientific Publications, 5, pp.143-175.

Malavear, M.Y.G., 2002. *Modeling the energetics of Steller sea lions (Eumetopias jubatus) along the Oregon coast*, Oregon State University, Corvallis. MSc thesis. URL: https://ir.library.oregonstate.edu/concern/graduate_projects/wd3761431

McLellan, W.A., Koopman, H.N., Rommel, S.A., Read, A.J., Potter, C.W., Nicolas, J.R., Westgate, A.J. and Pabst, D.A., 2002. Ontogenetic allometry and body composition of harbour porpoises (Phocoena phocoena, L.) from the western North Atlantic. Journal of Zoology, 257(4), pp.457-471.

Nabe-Nielsen, J., Tougaard, J., Teilmann, J., Lucke, K., Forchhammer, M., 2013. How a simple adaptive foraging strategy can lead to emergent home ranges and increased food intake. Oikos 122, 1307–1316.

Nabe-Nielsen, J., Sibly, R.M., Tougaard, J., Teilmann, J. and Sveegaard, S., 2014. Effects of noise and by-catch on a Danish harbour porpoise population. Ecological Modelling, 272, pp.242-251.

Nabe-Nielsen, J., van Beest, F.M., Grimm, V., Sibly, R.M., Teilmann, J. and Thompson, P.M., 2018. Predicting the impacts of anthropogenic disturbances on marine populations. Conservation Letters, 11(5), p.e12563.

NIRAS, Rambøll, and DHI, 2015. Underwater noise and marine mammals. Technical Report from Energinet.dk No. 15/06201-1. Rev. nr. 4. URL: https://naturstyrelsen.dk/media/162585/underwater-noise-and-marine-mammals_2392023_rev4.pdf

Oftedal, O. T. 1997. Lactation in whales and dolphins: evidence of divergence between baleen and toothed species. Journal of Mammary Gland Biology and Neoplasia 2(3):205-230.

Otani, S., Naito, Y., Kato, A. and Kawamura, A., 2001. Oxygen consumption and swim speed of the harbor porpoise Phocoena phocoena. Fisheries science, 67(5), pp.894-898.

Parry, D. A. 1949. The structure of whale blubber, and a discussion of its thermal properties. Journal of Cell Science 3(9):13-25.

Pinheiro, J., Bates, D., DebRoy, S. and Sarkar, D., 2019. R Core Team (2017) *nlme: linear and nonlinear mixed effects models*. R package version 3.1-139. Computer software: Retrieved from https://CRAN. R-project. org/package= nlme

Prentice, A.M. and Prentice, A., 1988. Energy costs of lactation. Annual review of nutrition, 8(1), pp.63-79.

Pullar, J.D. and Webster, A.J.F., 1977. The energy cost of fat and protein deposition in the rat. British Journal of Nutrition, 37(3), pp.355-363.

R Core Team., 2019. R: A language and environment for statistical computing. R Foundation for Statistical Computing, Vienna, Austria. http://www.R-project.org/

Read, A.J. and Hohn, A.A., 1995. Life in the fast lane: the life history of harbor porpoises from the Gulf of Maine. Marine Mammal Science, 11(4), pp.423-440.

Rechsteiner, E.U., Rosen, D.A. and Trites, A.W., 2013. Energy requirements of Pacific white-sided dolphins (Lagenorhynchus obliquidens) as predicted by a bioenergetic model. Journal of Mammalogy, 94(4), pp.820-832.

Rojano-Doñate, L., McDonald, B.I., Wisniewska, D.M., Johnson, M., Teilmann, J., Wahlberg, M., Højer-Kristensen, J. and Madsen, P.T., 2018. High field metabolic rates of wild harbour porpoises. Journal of experimental biology, 221(23), p.jeb185827.

Ryg, M., Smith, T.G. and Øritsland, N.A., 1988. Thermal significance of the topographical distribution of blubber in ringed seals (*Phoca hispida*). Canadian Journal of Fisheries and Aquatic Sciences, 45(6), pp.985-992.

Ryg, M., Lydersen, C., Knutsen, L.Ø., Bjørge, A., Smith, T.G. and Øritsland, N.A., 1993. Scaling of insulation in seals and whales. Journal of Zoology, 230(2), pp.193-206.

SCANS-III, 2016. Small Cetaceans in the European Atlantic and the North Sea (SCANS-III). Final Report. University of St Andrews, UK. http://biology.st-andrews.ac.uk/scans3/.

Scheffer, M., Baveco, J.M., DeAngelis, D.L., Rose, K.A. and van Nes, E., 1995. Super-individuals a simple solution for modelling large populations on an individual basis. Ecological modelling, 80(2-3), pp.161-170.

Sibly, R.M., Brown, J.H. and Kodric-Brown, A. eds., 2012. *Metabolic ecology: a scaling approach*. John Wiley & Sons.

Sibly, R.M., Grimm, V., Martin, B.T., Johnston, A.S., Kułakowska, K., Topping, C.J., Calow, P., Nabe-Nielsen, J., Thorbek, P. and DeAngelis, D.L., 2013. Representing the acquisition and use of energy by individuals in agent-based models of animal populations. Methods in Ecology and Evolution, 4(2), pp.151-161.

Sørensen, T.B. and Kinze, C.C., 1994. Reproduction and reproductive seasonality in Danish harbour porpoises, Phocoena phocoena. Ophelia, 39(3), pp.159-176.

Sveegaard, S., Teilmann, J., Tougaard, J., Dietz, R., Mouritsen, K.N., Desportes, G. and Siebert, U., 2011. High-density areas for harbor porpoises (Phocoena phocoena) identified by satellite tracking. Marine Mammal Science, 27(1), pp.230-246.

Tanaka, H., Li, G., Uchida, Y., Nakamura, M., Ikeda, T., Liu, H. 2019. Measurement of time-varying kinematics of a dolphin in burst accelerating swimming. PLoS ONE 14(1): e0210860. https://doi.org/10.1371/journal.pone.0210860

Thompson, P.M., Brookes, K.L., Graham, I.M., Barton, T.R., Needham, K., Bradbury, G. & Merchant, N.D. 2013. Short-term disturbance by a commercial two-dimensional seismic survey does not lead to long-term displacement of harbour porpoises. - Proceedings of the Royal Society B-Biological Sciences 280:8.

Turchin, P., 1998. Quantitative analysis of movement. Sinauer.

Urick, R.J., 1983. Propagation of sound in the sea: Transmission loss, I and II. Principles of underwater sound. McGraw-Hill Inc, New York, pp.177-179.

Van Moorter, B., Visscher, D., Benhamou, S., Börger, L., Boyce, M.S. and Gaillard, J.M., 2009. Memory keeps you at home: a mechanistic model for home range emergence. Oikos, 118(5), pp.641-652.

Worthy, G. A., and E. F. Edwards. 1990. Morphometric and biochemical factors affecting heat loss in a small temperate cetacean (Phocoena phocoena) and a small tropical cetacean (Stenella attenuata). Physiological Zoology 63(2):432-442.

Worthy, G.A., 1991. Insulation and thermal balance of fasting harp and grey seal pups. Comparative Biochemistry and Physiology Part A: Physiology, 100(4), pp.845-851.